

UNIVERSITY OF PÉCS

Doctoral School of Chemistry

**Encapsulation of sulfamethazine drug by  $\beta$ -cyclodextrins  
and its adsorption on carbon nanotubes**

**PhD thesis**

**Hiba Mohamedameen**

Supervisor:

**Beáta Lemli**

Assistant professor

Pécs

2020

# Abstract

Sulfonamides are preventive and therapeutic agents for certain infections caused by gram-positive and gram-negative microorganisms. At the same time, their widespread application is hindered by their low solubility in aqueous media. Since the water solubility of sulfonamide drugs is increased in the presence of cyclodextrins, the host-guest type complex formation of these antibiotics with cyclodextrins is an extensively studied field.

Sulfamethazine is a representative member of the sulfonamide antibiotic drugs, it is still used in human and veterinary therapy. Previous studies described the ability of  $\beta$ -cyclodextrin to increase the solubility of this drug in aqueous solution and studied the structure of the complexes by experimental and molecular modeling techniques. This work aims to examine the interactions of sulfamethazine with two  $\beta$ -cyclodextrin derivatives at different pH in the temperature range of 298-313 K. Results showed the formation of stable complexes of sulfamethazine with both native and randomly methylated  $\beta$ -cyclodextrin host molecules. Spectroscopic measurements and molecular modeling studies indicated the possible driving forces (hydrophobic interaction, hydrogen bonding, and electrostatic interaction) of the complex formation, and highlighted the importance of the reorganization of the solvent molecules during the entering of the guest molecule into the host's cavity. Functionalization of the  $\beta$ -cyclodextrin molecule does not affect considerably the complex stabilities, therefore the native  $\beta$ -cyclodextrin molecule looks the simplest and most effective inclusion host to design a selective and sensitive tool for sulfamethazine detection. The protonation state of this drug affects not only its aqueous solubility but controls its inclusion complexes with  $\beta$ -cyclodextrins. The pH-affected structures of the complexes explain previous contradictory findings based on the inclusion of the aniline moiety as well as the pyrimidine ring through the cyclodextrin cavity. Furthermore, surprisingly, the interaction between the neutral and anionic forms of the guest molecule and cyclodextrins with electron rich cavity is thermodynamically more favorable compared to the cationic guest. This

property probably due to the enhanced formation of the zwitterionic form of sulfamethazine in the hydrophobic cavities of cyclodextrins, which affect significantly the stability of sulfamethazine - cyclodextrin complexes.

Since sulfonamide antibiotics, including sulfamethazine, are poorly metabolized, they can be found in surface water, in wastewater and in meat-producing animals with considerable concentrations. Therefore, several studies have focused on the sulfonamide drugs adsorption on different kinds of natural and synthetic materials to remove them from the environment. Accordingly, in this work, the removal of sulfamethazine from water has also been tested. Based on the interaction between sulfamethazine and  $\beta$ -cyclodextrin, a cyclodextrin containing insoluble polymer has been tested to extract sulfamethazine from aqueous solution. Furthermore, carbon nanotubes, successfully used for the adsorption of several antibiotics earlier, have also been investigated as possible sorbents to eliminate this drug from aqueous solution. Systematic analysis has been done to describe the effect of the number of layers of walls and the effect of the functionalization of the carbon nanotubes. Results showed that although insoluble  $\beta$ -cyclodextrin bead polymer is not applicable for removing sulfamethazine from aqueous solution effectively, single-walled carbon nanotubes are suitable for extracting this antibiotic from aqueous media.

These observations might be relevant for the preparation of orally administered products of sulfonamide-cyclodextrin complexes which can be useful in finding materials suitable for developing new sulfonamide drug binders to remove these drugs from contaminated beverages, e.g. from drink water.

## Abbreviations

**AM1** Austin Model 1

**CD** Cyclodextrin

**BCD**  $\beta$ -Cyclodextrin

**BBP**  $\beta$ -Cyclodextrin Bead Polymer

**C-MWCNTs** Carboxyl Functionalized Multi-Walled Carbon Nanotubes

**CNTs** Carbon Nanotubes

**DWCNTs** Double-Walled Carbon Nanotubes

**GC-MS** Gas Chromatography-Mass Spectrometry

**H-MWCNTs** Hydroxyl Functionalized Multi-Walled Carbon Nanotubes

**HPLC** High Performance Liquid Chromatography

**FT-IR** Fourier Transform Infrared Spectroscopy

**K** Binding Constant

**LC-MS** Liquid Chromatography-Mass Spectrometry

**M** Concentration unit, mol/L

**MeOH** Methanol

**MWCNTs** Multi-Walled Carbon Nanotubes

**NMR** Nuclear Magnetic Resonance Spectroscopy

**PL** Photoluminescence

**RAMEB** Randomly Methylated  $\beta$ -Cyclodextrin

**SMT** Sulfamethazine

**SWCNTs** Single-Walled Carbon Nanotubes

**UV-Vis** Ultraviolet-Visible

$\Delta G$  Gibbs Free Energy Change

$\Delta H$  Enthalpy Change

$\Delta S$  Entropy Change

# Contents

<b>1</b>	<b>INTRODUCTION.....</b>	<b>1</b>
1.1	Cyclodextrins.....	2
1.2	$\beta$ -Cyclodextrin bead polymers .....	5
1.3	Carbon nanotubes, a nanoscale allotrope of carbon .....	5
1.4	Sulfonamides, a group of synthetic antibiotics .....	10
1.5	The previous results of the recent works.....	12
1.6	Characterization of the complexation of SMT drugs by cyclodextrins and SMT adsorption on carbon nanotubes.....	16
1.6.1	Fluorescence spectroscopy .....	16
1.6.2	Ultraviolet and visible absorption spectroscopy .....	17
1.6.3	Fourier transform infrared spectroscopy .....	17
1.6.4	High Performance Liquid Chromatography.....	17
1.6.5	Molecular modeling.....	17
<b>2</b>	<b>OBJECTIVE .....</b>	<b>18</b>
<b>3</b>	<b>EXPERIMENTS.....</b>	<b>19</b>
3.1	Materials and methods .....	19
3.1.1	Materials.....	19
3.1.2	Instruments .....	19
3.1.2.1	UV–Vis spectrophotometry .....	19
3.1.2.2	Fluorescence spectroscopic studies.....	20
3.1.2.2.1	Determination of the complex stabilities at room temperature .....	20
3.1.2.2.2	Temperature-dependent measurements of SMT-BCD and SMT-RAMEB... ..	20
3.1.2.2.3	Measurement of SMT adsorption on CNTs measurements .....	20
3.1.2.3	Fourier transform infrared spectroscopy.....	20
3.1.2.4	High performance liquid chromatography .....	20
3.2	Sample preparations .....	21
3.2.1	Phosphate buffer .....	21
3.2.2	The aqueous solution of the complexes .....	21
3.2.3	Adsorption of SMT on BBP and CNTs.....	21
3.2.4	Adsorption isotherms .....	21
3.2.5	Statistical Analyses .....	22
3.3	Molecular modeling studies.....	22
3.3.1	Determination the geometries of SMT and BCD .....	22

3.3.2	Determination of the thermodynamic parameters of the SMT-BCD or SMT-RAMEB complexes.....	23
<b>4</b>	<b>RESULTS AND DISCUSSIONS.....</b>	<b>26</b>
4.1	The protonation states of SMT molecule .....	26
4.1.1	Optical spectroscopic properties of SMT .....	27
4.1.2	Protonation states and structures of SMT molecule .....	29
4.2	Inclusion complex formation between SMT and CDs.....	30
4.2.1	Complexation stabilities of SMT– BCD and SMT-RAMEB at varying pH .....	30
4.2.2	The possible structures of SMT- BCD and SMT- RAMEB complexes.....	33
4.2.3	Thermodynamic studies .....	35
4.2.4	Driving forces of the complex formation SMT and BCDs .....	39
4.3	SMT removal from aqueous solutions by water insoluble nanomaterials .....	43
4.3.1	Adsorption behavior and mechanisms.....	44
4.3.2	Adsorption of SMT by insoluble BCD bead polymer .....	45
4.3.3	Adsorption of SMT onto insoluble CNTs .....	46
4.3.3.1	Adsorption isotherm of SMT on the CNTs.....	48
<b>5</b>	<b>CONCLUSIONS.....</b>	<b>53</b>
<b>6</b>	<b>REFERENCES .....</b>	<b>56</b>
<b>7</b>	<b>Appendix .....</b>	<b>71</b>
<b>8</b>	<b>Publication List .....</b>	<b>75</b>
<b>9</b>	<b>Acknowledgements.....</b>	<b>77</b>

# Chapter 1

---

## 1 Introduction

Host-guest interaction has become a very common expression in organic, analytical, inorganic, biological and physical chemistry. In general, it can be defined as supramolecular aggregates between large molecules that have a specific shape (host or receptor) and smaller molecules (guest or analyte), that are stabilized by multiple non-covalent bonds such as hydrogen bond,  $\pi$ - $\pi$  stacking, cation- $\pi$  bond, Coulomb interaction, electrostatic and hydrophobic interactions. Encapsulation occurs when a guest molecule is entrapped inside the macrocyclic cavity of a host molecule [1,2]. Supramolecular chemistry is a powerful approach to study nanostructures that mimic the sophisticated biological systems. A major type of macrocyclic compounds is cyclodextrins (CDs), which were selected as host molecules due to their good selectivity and sensitivity [3].

Nanomaterials, such as nanoparticles, nanotubes, nanorods, nanofibers and nanoribbons, have attracted much attention in the past few years due to their potential applicability in medicine and biology. The overall dimensions of these materials are in the nanoscale, where usually at least one of the dimensions is under 1000 nm. There are some important size-dependent properties of these nanomaterials that are already known, however, wide application still seems to be a big challenge and requires further investigations. The field of carbon nanotubes (CNTs) is considered to be a revolutionary research field presently. Various CNTs having been used for the adsorption of aqueous heavy metals and drugs for reducing environmental pollution [4] attracted the attention of scientists

Sulfonamides (SAs) are the first synthesized antimicrobial drugs and are still in use today. These antibiotics are widely used to treat human and animal diseases. Sulfamethazine (SMT) is one of the most important members of the SA drug family and it is used for the treatment of bacterial infections including those causing



bronchitis or urinary tract infections. Unfortunately, residues of SMT were found in surface water and wastewater and in meat-producing animals [5].

## 1.1 Cyclodextrins

The credit for the development of supramolecular chemistry must go to Lehn, Cram, and Pedersen who won the Nobel Prize of 1987 for their leading discoveries in the host-guest systems. A series of macrocyclic molecules and their derivatives have been investigated during the past few decades, including calixarenes, crown ethers, CDs, cyclophanes, cucurbit[n]urils, and others [6] (Figure 1). These macrocyclic molecules play the host role, possessing the cavities that encapsulate the guests [7].

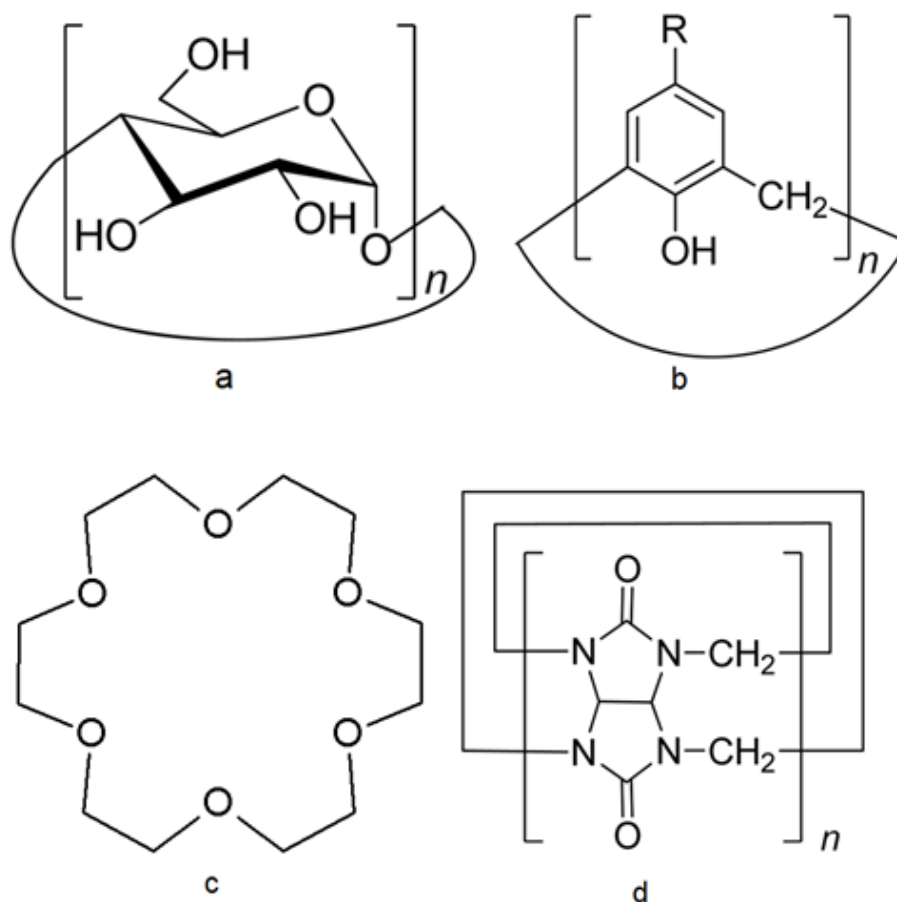


**Figure 1** Chemical structures of some macrocyclic molecules: a) CDs, b) calixarenes, c) 18-crown 6-ether and d) cucurbit[n] urils, a,b,d are cited from Ref. 6

In 1891 Villiers [8] discovered CDs, which have undergone extensive studies to this date. The synthesis of CDs is relatively easy because they can be prepared from starch precursors, like potato, rice, corn and by enzymetriggered starch degradation [9]. These synthesized CDs are inexpensive and can have a wide range of applications in various fields such as analytical chemistry [10], enzyme technology [11], catalytic reactions [12], and pharmaceuticals [13]. The pharmaceutical uses of CDs have been discussed in numerous reviews and books [14- 18]. The concept of CDs was a major subject of a biennial International Cyclodextrin Symposium and in the Society of Cyclodextrins in Japan [19]. CDs are 1 - 4 R-linked cyclic oligomers of anhydro-glucopyranose [20]. The shape of CD can be toroidal with the secondary hydroxyl groups at the wide side and the primary hydroxyl groups at the narrow side [7]. They are composed of 6, 7 or 8 glucose subunits called  $\alpha$ -,  $\beta$ - (BCD) and  $\gamma$ -CD, respectively (Figure 2). The depth of the hollow cavity is 0.78 nm for all three types of CDs.

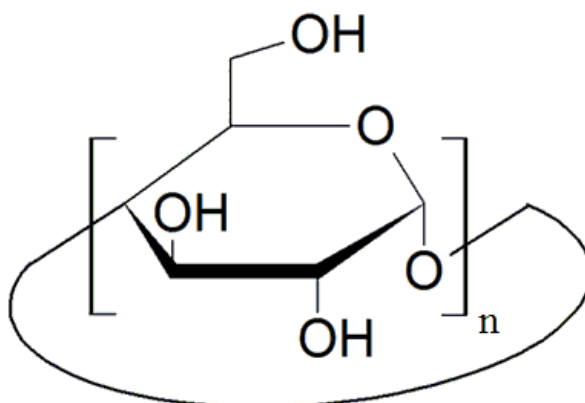


**Figure 2** Chemical structure of CD. n=6, 7, 8 for  $\alpha$ -CD, BCD,  $\gamma$ -CD respectively, cited from Cyclolab Ltd

The hydroxyl groups of the glucose units are oriented toward the outside at the orifice of the two ends. A variety of guests can be encapsulated into the cavity via the host–guest interaction. CDs with hydrophilic external surfaces and hydrophobic hollow cavities in aqueous conditions and even in the solid-state enable the inclusion of small molecules [21], cationic or anionic guests [22], proteins [23] and polymer chains [24].

Hydrophobic and van der Waals interactions between the inner surface of the CD ring and the hydrophobic sites of the guest molecule are the main driving forces for

the formation of CD inclusion compounds [25]. Researchers studied the binding constant of a CD inclusion compound with the guest which can be enhanced by dipole-dipole moment interaction, e.g., dipole moments induced on  $\alpha$ -CD-*p*-NP higher than  $\alpha$ -CD-H<sub>2</sub>O and  $\alpha$ -CD-MeOH [26]. Modified CDs such as randomly methylated  $\beta$ -cyclodextrin (RAMEB), 2-hydroxypropyl  $\beta$ -cyclodextrin and heptakis (2,3,6-tri-O-methyl)- $\beta$ -cyclodextrin have improved solubility and gave an excellent safety profile compared to the native BCD (Figure 3).

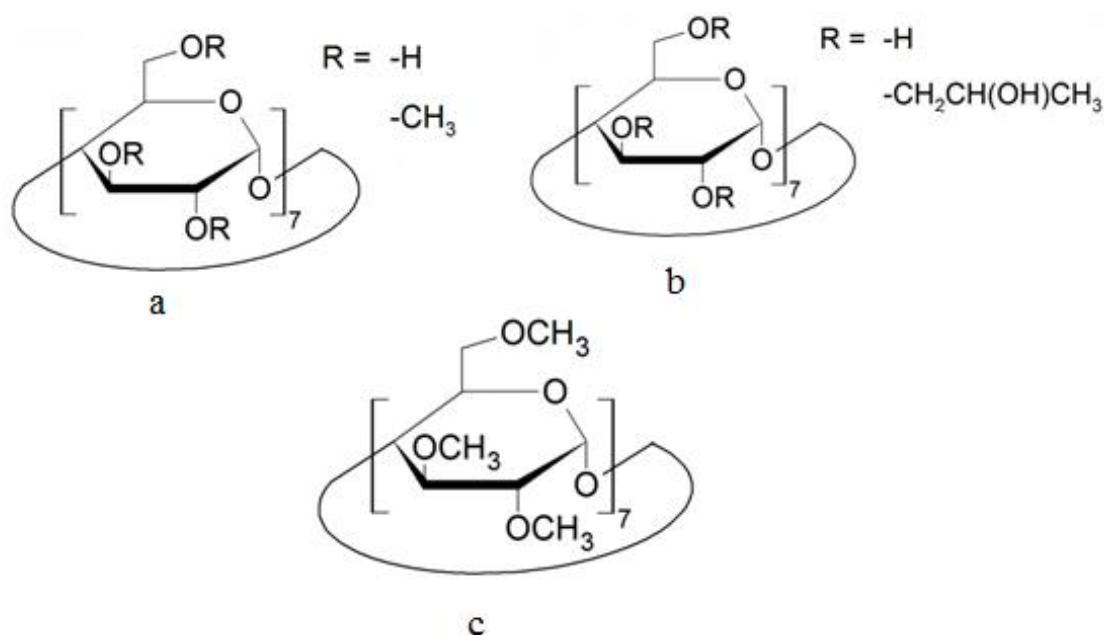


**Figure 3** Chemical structure of modified CDs a) RAMEB, b) 2-hydroxypropyl  $\beta$ -cyclodextrin, c) heptakis (2,3,6-tri-O-methyl)- $\beta$ -cyclodextrin, cited from Cyclolab Ltd

CDs offer several advantages compared to other cavity-shaped molecules. Extensive studies on the use of CDs in the biomedical field were fostered by the properties of the natural availability in starch, leading CDs to exhibit good water solubility, good biocompatibility, and nontoxicity toward biological systems and availability in large quantities [27]. The construction of CD-based supramolecular nanoparticles or aggregates in nanoscale size has received great attention from researchers [28,29]. Due to their various reversibly buildable blocks, this type of supramolecular system has been used under different conditions in various morphologies such as ribbons, orderly patterned threads, tubes and vesicles, with diagnostic and therapeutic

applications [30]. widespread applications in the biomedical field such as bioimaging using these supramolecular systems have been reported [31,32]. Several efforts have been made to introduce catalytic groups onto CDs to build artificial enzymes for biomimetic reactions after obtaining the evidence of using CDs as enzyme models [33,34]. Encapsulation of aromatic oily plant extracts by CDs can increase physiochemical stability and aqueous solubility of these essential oils, potential food preservatives. Both stability and selectivity of CD inclusion complexes can be strongly affected by chemical modifications of parent molecules [35]. Furthermore, sensitive dye molecules or molecular wires can be protected against decomposition by rotaxation within CD cavities. CDs can be functionalized by a wide variety of synthetic methods [36,37], and they are sometimes chosen for developing drug delivery systems. The formation of host–guest complexes between drugs and CDs or CD derivatives greatly increases the water solubility of hydrophobic drugs, thus enhancing drug availability in biological systems [38].

## **1.2 $\beta$ -Cyclodextrin bead polymers**

Polymer beads containing BCD ( $\beta$ -cyclodextrin bead polymers - BBP) are prepared through crosslinking of CD molecules and functional linking agents. This is a highly effective technique for manipulating CD functionality and gives important properties such as stability toward heat, pH and water insolubility. Therefore, BBP can be used in many applications as adsorbent material to remove the organic pollutants and heavy metal ions from water [39] including the removal of phenol from wastewater [40], and they also effectively adsorb alternariol from aqueous solutions [41].

## **1.3 Carbon nanotubes, a nanoscale allotrope of carbon**

The concept of allotropy is defined as the capability of some chemical elements to configure a range of different molecular structures from the same type of atoms. The chemical and physical properties of the allotropy have been investigated with regard to the structural geometry of the atoms and the type of chemical bonds within the molecules. One of the most interesting elements is carbon, which is available in several structures with different properties. In science, technology and human life

there are two different types of hard carbon allotropes including diamond and graphite [42].

Over the last decades of the 20<sup>th</sup> century, several new low-dimensional carbon forms have been discovered by the Japanese researcher S. Iijima [43] who called the attention to the helical microtubules yielding numerous types of carbon allotropes. The novel materials involving graphene, graphite, CNTs and fullerenes have attracted considerable attention [44,45] (Figure 4). Since that time on CNTs have been developed into a major field of research and currently they are at the cutting edge of material science research in nanotechnology, materials science and electronics [46].

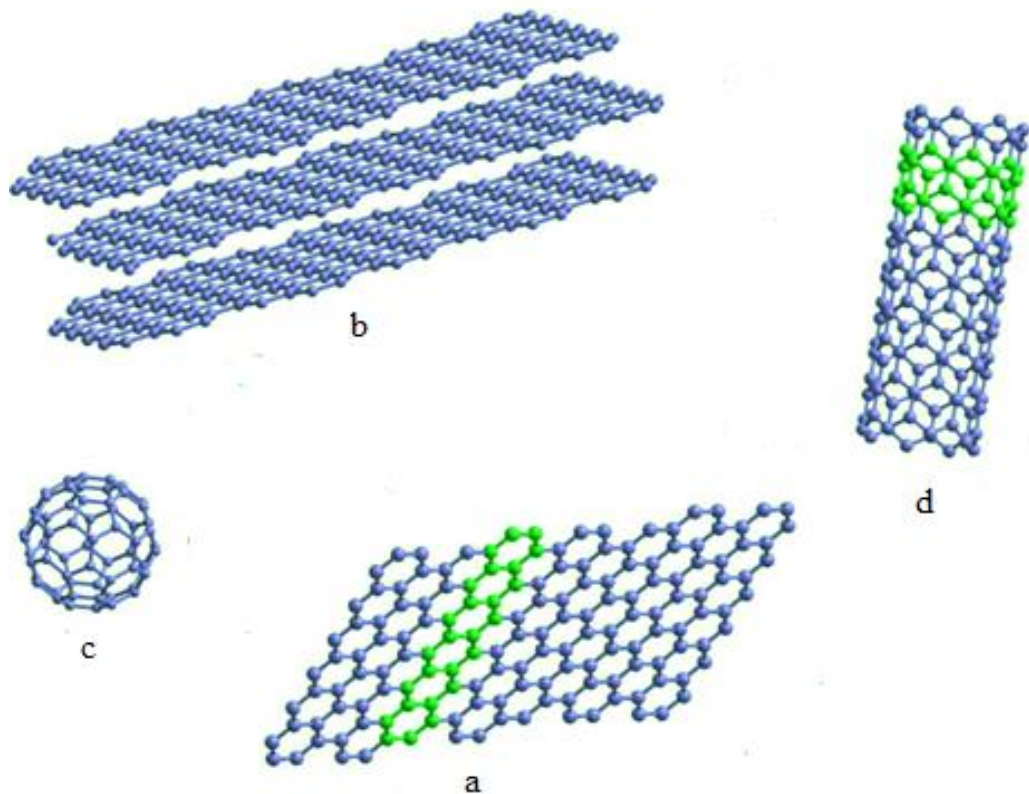


**Figure 4** Carbon nanostructures a) Grafene, b) grafene layers, c) fullerene and d) carbon nanotube

CNTs are cylindrical tubes made up by hexagonally arranged  $sp^2$ -hybridized carbon atoms with an inner diameter of several nanometers ( $> 0.9$  nm), and a length of a few micrometers [47]. CNTs can be classified as single cylinder known as single-walled

carbon nanotubes (SWCNTs) with a diameter around 1–3 nm and a length of a few micrometers, isolate double-walled carbon nanotubes (DWCNTs) with a diameter less than 5 nm and a length around 10  $\mu\text{m}$ , also multi-cylinders with coincided centers known as multi-walled carbon nanotubes (MWCNTs) with a diameter of 5–40 nm and a length around 10  $\mu\text{m}$  [48] (Figure 5). Additionally, there are functionalized CNTs, such as, hydroxyl functionalized multi-walled carbon nanotubes (H-MWCNT) and carboxyl functionalized multi-walled carbon nanotubes (C-MWCNT) [49] (Figure 6).

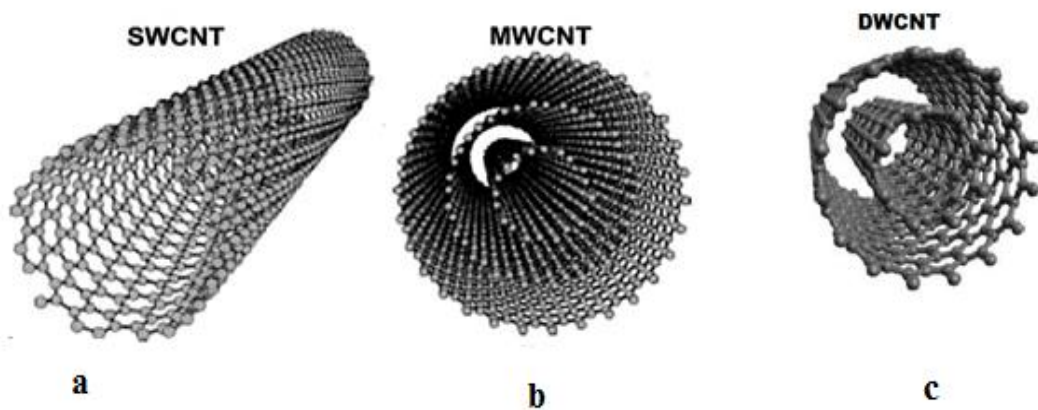


**Figure 5** Carbon nanotubes a) SWCNT, b) MWCNT and c) DWCNT

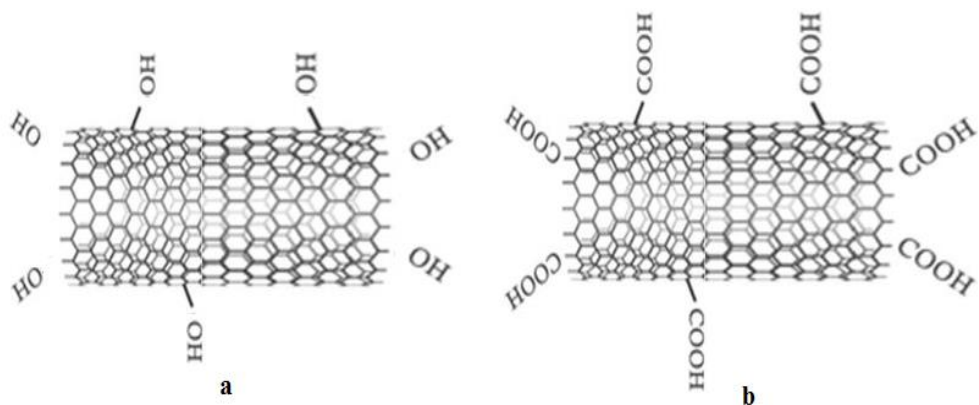


**Figure 6** Functionalized MWCNTs a) H-MWCNTs and b) C-MWCNTs

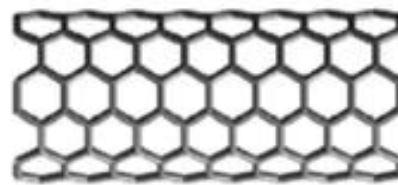
SWCNTs have larger ratios compared to MWCNTs due to their smaller diameter. Moreover, the aspect ratios for all CNTs appear much higher (length to diameter ratios) than other materials [50]. The modification of the tubes' structures themselves requires high temperatures to change from a SWCNT to a DWCNT or even to a

MCWNT. Structures and properties of CNTs are usually utilized in obtaining the designs which perform multiple synergistic functions or solve a specific problem [51]. The electrical properties of SWCNTs depend on their chirality or hexagon orientation regarding the tube axis which is wrapped by the graphene plane, thus, there are three shapes of SWCNTs (Figure 7):

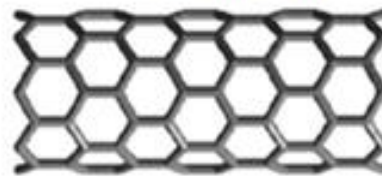
1. Armchair (electrical conductivity > copper)
2. Zigzag (semi-conductive properties)
3. Chiral (semi-conductive properties)

Various sub-configurations can be obtained by shifting the wrapping axis from the zigzag plane toward the armchair plane [52]. The transfer of semiconductor zigzag (7,0) and metallic armchair (4,4) SWCNTs have no significant difference in their vibration dynamics properties in the temperature range of 278-378 K [53].

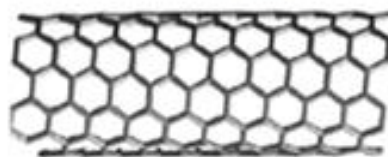
On the other hand, multiple carbon layers, frequently with variable chirality are involved in MWCNTs, producing extraordinary mechanical properties instead of outstanding electrical characteristics [50]. Accordingly, CNTs show high thermal and electrical conductivity compared to other conductive materials. Additionally, they can reduce heavy metals and improve the adsorptive capacity [54,55]. It is possible to obtain the structure of CNTs with a distinct combination of rigidity, strength and elasticity. This tailoring is an important characteristic as compared to other fibrous materials. The magnetic properties, separation and recycling of the nanomaterials have been facilitated [51]. A huge leap in the diverse applications in the medical, industrial and technical fields has been made due to the unique electronic, thermal, and outstanding mechanical stability and electric transport capacity, especially the transport of ions and molecules in the nanoscales channel of CNTs [56-59].



**a Armchair**



**b Zigzag**



**c Chiral**

**Figure 7** Single-walled carbon nanotube a) armchair, b) zigzag and c) chiral

Another important property of CNTs is that they are not soluble in most of the popular solvents such as phenol and benzene, but these aromatic molecules can adsorb onto the surfaces of the CNTs [60]. Salipira *et al.* removed organic pollutants from water with CNTs and CD polymers [61]. Furthermore, CNTs also adsorb heavy metals, such as mercury, lead, chromium and cadmium which are regarded as non-biodegradable, bioaccumulative and extremely dangerous. These metals produce



hazardous threats to plant, animal, and human health, even at trace levels of concentration [62,63]. Furthermore, the adsorption properties of suspended CNTs, beside their exposed surface area, play an important part in adsorbing organic compounds such as SA drugs and removing them from aqueous solutions [64].

## 1.4 Sulfonamides, a group of synthetic antibiotics

Antibiotics have been widely used and are currently in the focus of interest due to the rapid therapeutic efficacy and preventive benefits to humans and animals [65]. In 1932, a German scientist Gerhard Domagk, while working for the chemical and dye company, I. G. Farben, discovered that a red dye compound, “Prontosil,” was effective in treating mice injected with *Streptococci*. Unfortunately, his ideas were not taken into consideration until 1935. The active ingredient in the dye compound was SA which was later tested by the Pasteur Institute in France, to justify Domagk’s idea [66]. Sulfa drugs or SAs are an important group of antibiotics. Generally, the concept refers to a group of drugs containing the chemical structure of sulfanilic amide groups, one of the most widely administered groups of antibiotics in human medicine and animal husbandry [1]. The European Food Safety Authority founded in 2002 by the European Union, implemented a farm-to-table approach in the European Union food legislation. Accordingly, they took into account several debates on the use of antibiotics, including SAs, as growth promoters [67]. The structure of SAs contains one basic amine group ( $-NH_2$ ) and one acidic amide group ( $-NH-$ ) which correspond to  $pK_{a1}$  and  $pK_{a2}$ ; respectively. It can accept a proton by the amine group and release a proton by the amide group under specific pH conditions [68]. Approximately 30 SAs have been investigated so far and some of them have a good antibacterial effect [69-71]. Figure 8 shows the most important SAs drugs (for some of SAs drugs and their  $pK_a$  values) see appendix.

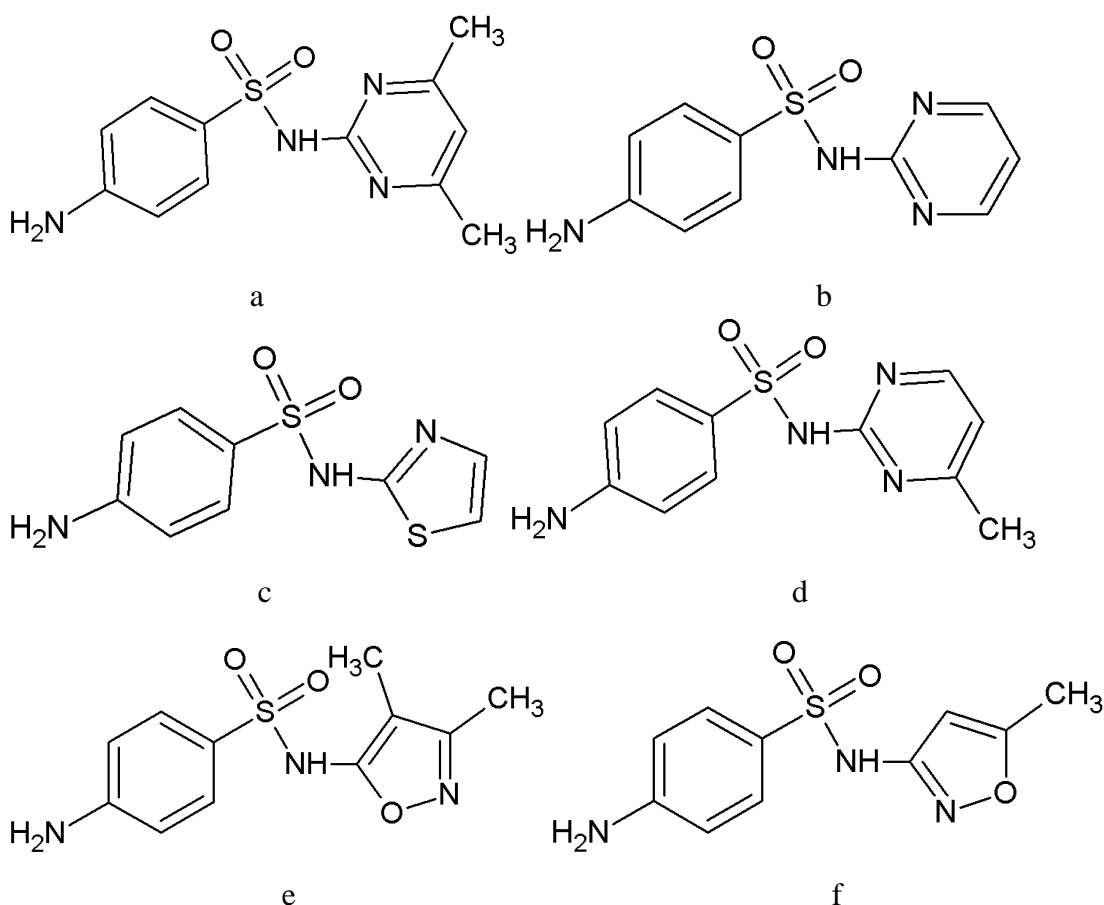


**Figure 8** Structure of some selected SA drugs a) SMT, b) sulfadiazine, c) sulfathiazole, d) sulfamerazine, e) sulfisoxazole and f) sulfamethazole

These drugs are preventive and therapeutic agents for certain infections caused by gram-positive and gram-negative bacteria, fungi and certain protozoa. SAs have the advantage of being available for a relatively low price [72,30]. SAs have a number of efficient applications such as anti-angiogenic [73], anti-tumor [74], anti-inflammatory and anti-analgesic [75] in human medicine and animal therapy including cattle, sheep, pigs and poultry [76]. They are used to cure infectious diseases of the digestive and respiratory systems and affections of the skin (in the form of ointments). Moreover, they are used for the prevention or therapy of coccidiosis in small domestic animals. SAs are also employed in hypoglycemic, antitumor, antiviral, diuretics and antithyroid agents [77]. Accordingly, sulfa drugs are considered powerful medicines (together with ampicillin and gentamycin) as chemotherapeutic agents to treat bacterial infections caused by *Escherichia coli* in

humans. SAs perform their antibacterial activity by the competitive suppression of dihydropterase enzyme towards the substrate P-amino benzoate [3].

SAs present unfavorable physicochemical properties such as poor aqueous solubility and dissolution rate, which is a major concern for its therapeutic use. Therefore, the popularity of SAs has decreased. New formulations with solubilizers to improve the efficacy and safety have been investigated in order to deliver the SAs to the targeted site. Moreover, the transfer of SA derivatives in the body can be controlled by encapsulation with carrier molecules. Among the candidates of molecular capsules BCD is used in the pharmaceutical industry as complexing agents [78]. pH-responsive host-guest encapsulation has increased attention not only in the field of material sciences but also in drug delivery systems [79].

SAs do not accumulate in humans because they are excreted after acetylation. Therefore, antibiotics in surface water, groundwater, and influent and finished water of municipal drinking water treatment have been discovered at relevant concentrations [80]. On the other hand, environmental antibiotics may come from municipal and agricultural origin [81]. SAs can be removed from the inorganic and organic pollutants by adsorbing in the large surface area of the insoluble CNTs [82].

## **1.5 The previous results of the recent works**

Although SAs are being clinically used since 1968, their therapeutic use still needs to be further addressed. Widely used in human and animal medicine, these drugs have low water solubility. One of the frequently applied strategies to enhance drug solubility is the complexation with CDs. In the past twenty years, several studies have demonstrated the improved solubility of SAs complexed by CDs compared to the free drug. 2-hydroxypropyl- $\beta$ -cyclodextrin seems to be a fruitful candidate to improve the aqueous solubility of SAs. The increased water solubility of sulfadiazine in the presence of 2-hydroxypropyl- $\beta$ -cyclodextrin has been reported [83]. The complexation of sulfisoxazole with hydroxypropyl- $\beta$ -cyclodextrin in itself improves the solubility of the pure drug, while the presence of triethanolamine has a beneficial effect on the solubilization process [84]. Furthermore, another formulation to enhance the water solubility of acetazolamide also based on the combined effect of

hydroxypropyl- $\beta$ -cyclodextrin and triethanolamine has been published [85]. However, the native and hydroxypropyl- $\beta$ -cyclodextrin are similarly effective to enhance the solubility of sulfamethizole [86]. While molecular encapsulation has become significant in pharmacology and drug delivery science, recent studies focus also on the stability of the SA drugs' complexes with CDs [1,87,88,72]. These studies state, that all tested different compounds, namely sulfamethoxazole, sulfisoxazole, sulfathiazole, sulfanilamide sulfamethizole, sulfamethazine, sulfadimethoxine, and sulfacetamide show similar affinity to BCD, the related association constant being  $\sim 10^3 \text{ M}^{-1}$ . Although these association constants are small, they are comparable with other inclusion complexes of CDs [89]. Furthermore, no significant difference has been found between the stability of sulfacetamide and sulfadimethoxine complexes with  $\alpha$ - or  $\beta$ -CD [87,72]. Furthermore, the complex structures also have been analyzed by combined nuclear magnetic resonance (NMR) spectroscopy and molecular modeling methods. The inclusion mode of sulfadiazine involves an  $\text{NH}_2$  orientation of the drug in the 2-hydroxypropyl- $\beta$ -cyclodextrin cavity [83], while, in the case of sulfamethizole, the guest molecule enters with its thiazole group into the CD cavity [86].

In the special case of SMT, Zoppi *et al.* investigated its increased solubility in the presence of CDs [90,78], while Bani-Yaseen and Mo'ala analyzed the complex formation in buffer-free aqueous media [1]. The aqueous solubility of SMT has been increased by its encapsulation with BCD [90] and methyl- $\beta$ -cyclodextrin [78]. Comparing the efficiency of solubility improvement under acidic and basic conditions with buffer-free solutions, the ionization of the SMT does not support the increase of its solubility. Although experimental results verified the formation of 1:1 inclusion complexes of SMT with both CDs, the affinity constant derived from phase solubility studies is higher in the case of the native BCD. At the same time, the functionalization of the host molecule does not affect the complexation mechanisms and the inclusion modes of the guest molecule. The spatial conformations of the complexes determined using NMR and molecular modeling studies show that SMT included the substituted pyrimidine ring into the CD cavity [90,78]. Contradicting to this, the result of another combined NMR and molecular modeling study [1] revealed that the encapsulation of SMT by BCD is favorable with the inclusion of the guest's

aniline moiety through the host's cavity. In this latter work, the association constant of SMT-BCD complex ( $\log K \sim 2.9$ ) in buffer-free aqueous solutions was also determined based on ultraviolet and visible spectroscopic studies.

Sulfonamide antibiotics are widely used in veterinary medicine all over the world, but most of the SAs fed to animals cannot be metabolized, therefore livestock feces and urine containing these antibiotics have created serious environmental pollution. An increasing number of papers focus on environmental pollution with sulfonamides [91]. Research extensively focuses not only on the possible risk of the pollution [92], but on the possible strategies for removing these veterinary antibiotics [93].

One of the possible removal techniques is adsorption. Based on the inclusion complexation of the small bioactive molecules with CDs the CD-containing BBP can effectively decrease the pollutant content of aqueous solution [40,41]. Furthermore, carbon nanotubes are reported to be promising adsorbents readily applicable in water and wastewater management. The optimization strategies of the removal of antibiotics from water using CNTs have been reported [94- 96]. The adsorption mechanism of SAs on CNTs is extensively investigated and strong adsorption affinity of CNTs for these antibiotics was found [97-100]. Comparative studies of graphite and MWCNTs have proved that these nanomaterials can be very promising and effective adsorbents for SA antibiotics [101]. They have especially focused on the investigation of the exact mechanism and predominant factors controlling the adsorption of SAs to MWCNT. The main driving force of the adsorption process is attributed to  $\pi$ - $\pi$  electron coupling with the graphene surface of the adsorbent. In addition to these results, similar pH dependence was observed in the case of both investigated carbon nanomaterials during the adsorption reaction and no considerable effect of the ionic strength was found. However, in the presence of dissolved soil humic acid the adsorption has been decreased dramatically, because of the competition for adsorbent surface area [101]. In contrast to this latter finding, Pan *et al.* have shown, that the presence of some humic acid can enhance the adsorption of organic materials, such as SAs [99]. Furthermore, 2 orders of magnitude higher adsorption of SAs onto humic acid-suspended CNTs than onto aggregated CNTs have been found. SA antibiotics often exist as differently charged species, depending on the pH, which makes more complicated to understand the exact mechanism of its

adsorption. Zhang *et al.* have been studied the adsorption contributions of different protonated states of various antibiotics to its total adsorption and the effect of the CNTs functionalization on the adsorption [102]. The pH dependent adsorption was well explained by hydrophobic and electron donor-acceptor interactions. However, the highest adsorption was achieved in acidic environment where the cationic form adsorbed to the surface by hydrogen bonds also had a dominant contribution. They examined the overlap of adsorption between SAs and other chemicals. Surprisingly, their results indicate, that bisphenol A concentration decreased the adsorption of the neutral antibiotic only, not the overall antibiotic concentration. In a freshly published article a carboxylic-functionalized carbon nanofibers- encapsulated Ni magnetic nanoparticles, a negatively charged CNT derivate and SA interaction was also examined [103]. Similarly to Zhang *et al.* [102], their study also emphasized electrostatic and  $\pi$ - $\pi$  interactions, as predominant driving forces for the adsorption of deprotonated SA, but they reported that in acidic solutions the mechanism of the adsorption is controlled by electrostatic interaction only. Tian *et al.* have investigated the adsorption of some selected SA species onto the surface of CNTs in aqueous solutions under various conditions [98]. Their findings have highlighted the special role of some physicochemical properties in controlling the removal of these SAs by an adsorbent. Isotherms showed that sonication-aided dispersion could enhance the efficiency of the sorption of the antibiotics on to the CNTs, due to the increased surface. However, the higher pH values of the solutions definitely decreased the adsorption capacity on the CNT surface of SAs, while the amount of the adsorbent had only minimal effect on the interaction.

The adsorption/desorption mechanisms on CNT surface have already been described in the literature in the case of most of the members of SA the family. Although, SMT shows a very complex and unconventional behavior, due to the fact that in aqueous environment it exists in four different forms (SMT<sup>0</sup>, SMT<sup>+</sup>, SMT<sup>-</sup> and insignificant amount of SMT<sup>±</sup>). Scientists also pay much attention to understanding the exact mechanism of SMT adsorption on carbon materials. Teixidó *et al.* have investigated the pH dependence of SMT adsorption on charcoal [104]. In strong acidic regions the protonated form with the positively charged surface implies  $\pi$ - $\pi$  donor-acceptor interaction, as the major driving force of the adsorption. Furthermore, the negatively

charged SMT especially in the alkaline region, coupled with the driving force between the aniline ring- and the  $\pi$ -electron rich graphene surface. another negative surface, where a proton exchange with water can occur, leading to the accumulation of  $\text{-OH}^-$  ions and resulting in a strong hydrogen-bond between  $\text{SMT}^0$  and carboxylate and phenolate groups on the surface. Furthermore, at pH 5, adsorption of  $\text{SMT}^0$  is followed by a partial proton release and results in a competition with triphenylammonium ion.  $\text{SMT}^+$  and/or  $\text{SMT}^\pm$  contributions enhanced by  $\pi^+-\pi$  electron donor-acceptor and Coulomb interactions have been highlighted. Yang *et al.* have proved the existence of pH and ionic strength dependent adsorption mechanism of SMT on MWCNTs, which can be mainly explained by electrostatic and hydrophobic interactions [105]. The presences of some anions and cations on SMT adsorption have been also analyzed. Results show that the adsorption is highly affected by the type of metal cations, the CNT and the pH applied, while anions insignificantly influence SMT adsorption on different CNT, even at various pH values.

## **1.6 Characterization of the complexation of SMT drugs by cyclodextrins and SMT adsorption on carbon nanotubes**

### **1.6.1 Fluorescence spectroscopy**

The fluorescence property undergoes significant changes upon complexation, providing an opportunity to study the weak molecular interaction between host and guest molecules by the highly sensitive fluorescence method. Analyzing the photoluminescence (PL) spectra of the host, the guest and their complex can determine both stoichiometry and association constant of the related process. Our team used this method to investigate several different types of complexes, e.g. resorcinarene derivatives – neutral phenol guest [106], malvidin – polyphenol [107], zearalenone – CDs [108].

### **1.6.2 Ultraviolet and visible absorption spectroscopy**

Ultraviolet and visible (UV–Vis) spectrophotometry is another useful method, furthermore easily available method for the detection of host-guest complexes. In the case of SAs it has been found that through the inclusion of the guest molecule inside the supramolecular cavity, its spectral characteristics can face notable changes enabling the determination of the stability constant of SA – CD complexes [1,72,38]. Besides that UV-Vis spectra are suitable to determine the  $pK_a$  values of different compounds, e.g. SAs [109].

### **1.6.3 Fourier transform infrared spectroscopy**

Fourier transform infrared (FT-IR) absorption bands changing in shape, shift and intensity can also clarify the host-guest complex formation. The encapsulation of SAs with CDs has also been validated by using this method [72,78].

### **1.6.4 High Performance Liquid Chromatography**

Several chromatography methods such as gas chromatography [110] gas chromatography/mass spectrometry [111], capillary electrophoresis [112], and liquid chromatography/mass spectrometry [113] are used to determine SAs in different samples. High performance liquid chromatography (HPLC) is also a suitable technique for the quantification of SAs, e.g. in honey [114,115], in chicken [116] or in aqueous solution [105].

### **1.6.5 Molecular modeling**

The computation of the host-guest complexes requires large resources. Fortunately, semi-empirical methods have been found to give accurate estimates of inclusion complex formation and complex properties [117,118]. In addition, a software to build and calculate theoretical models of CDs derivatives and their inclusion complexes also have been reported [119].



# Chapter 2

---

## 2 Objective

Previous studies described the capability of BCD for increasing the solubility of SMT in aqueous solution and investigated the structure of the complexes by experimental and molecular modeling techniques. However, contradictory results of the complex conformation have been reported. The present work aims to get a deeper look into the biologically important interactions of SMT drug with native and randomly methylated BCDs to explain the inclusion complex stability and the stoichiometry in aqueous solutions under different environments. The effects of pH and temperature on the host-guest system will also be analyzed. The thermodynamic parameters will be investigated both with experimental methods and molecular modeling.

The interactions between SAs and CNTs have attracted great attention, due to the serious ecological risks of these antibiotics. Since SMT is one of the serious environmental pollutants, in this work, the removal of SMT from water also will be tested. Based on the interaction between SMT and BCD, a CD containing insoluble polymer will be investigated to extract sulfamethazine from aqueous solution. Furthermore, CNTs, earlier successfully used for the adsorption of several antibiotics, will also be investigated as possible sorbents to remove this drug from aqueous solution. Systematic analysis will be done to describe the effect of the number of layers of walls and the effect of the functionalization of CNTs.

# Chapter 3

---

## 3 Experiments

### 3.1 Materials and methods

#### 3.1.1 Materials

SMT was purchased from Alfa Aesar. BCD, RAMEB and BBP (BCD content in the BBP: 50 m/m%) were obtained from CycloLab Cyclodextrin Research & Development Laboratory Ltd (Budapest, Hungary). SWCNTs, DWCNTs, MWCNTs, H-MWCNTs and C-MWCNTs were purchased from Guangzhou Heji Trade Co. (China). The tubes' average diameters are 1-2, 1.3-3, < 8, < 8 and < 8 nm and they are about 50, 15, 50, 50 and 50 microns in length with the purity of more than 90%, 50%, 95%, 95% and 95% in the case of SWCNTs, DWCNTs, MWCNTs, H-MWCNTs and C-MWCNTs, respectively. Methanol (spectroscopic grade) was purchased from Reanal. All the other analytical grade chemicals were purchased from VWR International Ltd (Debrecen, Hungary). Phosphate buffers with different pH (2- 10) were prepared in ultrapure water (conductivity < 0.1  $\mu$ S/cm, Adrona water purification system).

#### 3.1.2 Instruments

##### 3.1.2.1 *UV-Vis spectrophotometry*

Specord plus 210 spectrophotometer (Analytik Jena, Germany) was used to record the UV-VIS spectra. Photon counting method with 0.1 s integration time at 3 nm bandwidths was used for data collection. The measurements were carried out at 298.2 K. Quartz cuvettes (Hellma, path length 1.0 cm) were used in the measurements. Phosphate buffers with different pH (2, 5, 7 and 10) were the solvent.

### **3.1.2.2 Fluorescence spectroscopic studies**

#### **3.1.2.2.1 Determination of the complex stabilities at room temperature**

Fluorolog  $\tau 3$  spectrofluorometer (Jobin-Yvon/SPEX, Longjumeau, France) was used to investigate the fluorescence spectra of the different solutions with high sensitivity. Photon counting method with 0.1 s integration time was used to collect the data. 4 nm were the bandwidth of the excitation and emission. The PL emission spectra were recorded using the excitation wavelengths of 280 nm. The measurements were carried out at 298.2 K. Acrylic cuvettes (Sarstedt, path length 1.0 cm) with right-angle detection were used in the measurements of the interactions between SMT and cyclodextrins.

#### **3.1.2.2.2 Temperature-dependent measurements of SMT-BCD and SMT-RAMEB**

Temperature-dependent steady-state fluorescence spectroscopic measurements were carried out at different temperatures: 298.2 K, 303.2 K, 308.2 K and 313.2 K. The PL emission spectra were recorded using the excitation wavelengths of 280 nm. Acrylic cuvettes (Sarstedt, path length 1.0 cm) with right-angle detection were used in the measurements of the interactions between SMT and CDs.

#### **3.1.2.2.3 Measurement of SMT adsorption on CNTs measurements**

Fluorescence spectroscopic measurements were carried out using 280 nm excitation wavelength at 298.2 K, for SMT with CNTs. Semi-micro quartz cell was used in the measurements of the interactions between SMT and carbon nanotubes.

#### **3.1.2.3 Fourier transform infrared spectroscopy**

SMT, BCD, RAMEB, SMT-BCD and SMT-RAMEB complexes fourier transform infrared spectra were recorded on Platinum Alpha T FT-IR (Bruker, Germany). Droplets of samples were used for these measurements. An average of ten scans with  $5\text{ cm}^{-1}$  resolution was applied.

#### **3.1.2.4 High performance liquid chromatography**

High Performance Liquid Chromatography (1100 HPLC, HP, Germany) with a UV detector equipment at 263 nm and reversed-phase  $C_{18}$  column (HP,  $5\ \mu\text{m}$ , 4.6 mm inner diameter x 150 mm length) was used to determine the area of SMT in the

supernatant. The retention time was 2.6 min. The injection volume was 20  $\mu\text{L}$ , the flow rate was 1  $\text{mL min}^{-1}$ . The volume ratio of the mobile phase was 50: 50 methanol and ultrapure water. This method is based on Yang *et. al.* [105], but the eluent composition was changed to obtain sufficient retention and baseline separation of SMT from the interfering peaks at the dead time.

## **3.2 Sample preparations**

### **3.2.1 Phosphate buffer**

The mixture of (0.1 M)  $\text{H}_3\text{PO}_4$  - (0.1 M)  $\text{Na}_2\text{HPO}_4$ , (0.01 M)  $\text{H}_3\text{PO}_4$  - (0.01 M)  $\text{Na}_2\text{HPO}_4$ , (0.01 M)  $\text{KH}_2\text{PO}_4$  - (0.01 M)  $\text{Na}_2\text{HPO}_4$  and (0.01 M)  $\text{KH}_2\text{PO}_4$  - (0.01 M)  $\text{NaOH}$  were prepared to reach the requested pH 2, 5, 7 and 10 respectively.

### **3.2.2 The aqueous solution of the complexes**

The stock solution of SMT (5000  $\mu\text{M}$ ) in methanol was prepared and stored at 277.2 K. For preparing the samples, appropriate volumes of the stock solution were evaporated under low pressure, then redissolved in phosphate buffers with different pH (2, 5, 7 and 10). The SMT concentration was (30  $\mu\text{M}$ ) in the absence and presence of BCD or RAMEB (0–3 mM).

### **3.2.3 Adsorption of SMT on BBP and CNTs**

SMT adsorption on BBP or CNTs was achieved by mixing standard amount (20  $\mu\text{M}$ ) of SMT in the presence of increasing amount (0.0-12.5 mg) of BBP and (0.0-0.5 mg) of CNTs in 1.5 ml buffered aqueous solution (pH 2, 5 and 7) at room temperature and stirring for (2 hours for BBP, 1 hour for CNTs). The insoluble BBP or CNTs were sedimented by pulse centrifugation (15000 rpm, 15 min) and gently 500  $\mu\text{l}$  supernatant was collected. Then the concentration of SMT in the supernatant was directly determined by HPLC and fluorescence emission.

### **3.2.4 Adsorption isotherms**

Varying quantities (2.5-100  $\mu\text{M}$ ) of SMT with 0.1 mg of BBP or CNTs in 1.5 ml buffered aqueous solution (pH 2, 5 and 7) at room temperature were stirred for 2 hours. The insoluble BBP or CNTs were sedimented by pulse centrifugation (15000

rpm, 15 min) and gently 500  $\mu$ l supernatant was collected. Then the concentration of SMT in the supernatant was directly determined by HPLC.

### 3.2.5 Statistical Analyses

Representing mean  $\pm$  SEM values of the data were calculated depending on three independent experiments. The One-Way ANOVA test was applied with Microsoft Excel used for statistical analyses. The significant level was set as 99% and  $p < 0.01$ .

## 3.3 Molecular modeling studies

Semiempirical AM1 (Austin Model) method was applied to determine the equilibrium geometry and the molecular interactions between the SMT molecules and the cyclodextrin derivatives were examined also experimentally. This semiempirical method was found to be sufficiently precise to determine at least the tendencies of the physical parameters along the interaction process and it offers an appropriate timeframe to examine such large systems as the SMT – BCD complexes. It must be mentioned here, that semiempirical methods can also implicitly consider the electron correlation. The interaction was examined along with the change of the Gibbs free energy, considering the entropy term through the molecular vibrations calculated in harmonic approximation.

### 3.3.1 Determination the geometries of SMT and BCD

During the synthesis of RAMEB, the methyl substituents were placed randomly. At the preparation of the model structure of this host all the OH groups were considered to be equivalent, thus at the lower or upper rim four or eight methyl groups were used to replace the hydrogen atoms of -OH groups [see details in Ref 89]. At the same time, in line with the experiences of Lemli *et al.* the CD derivatives (RAMEB, randomly methylated  $\gamma$ -CD, quaternary ammonium BCD, quaternary ammonium  $\gamma$ -CD) can be considered as charged species of the native molecules [41,120]. Accordingly, the electron donating property of the methyl groups can be considered as negatively charged BCD or  $\gamma$ -CD skeleton, while the electron withdrawing character of quaternary ammonium moieties can be considered as the positively charged BCD or  $\gamma$ -CD skeleton. However, to confirm that neglecting methyl groups

does not affect the entropy term, Lemli *et al.* performed calculations for the entropy change subtracting the entropy content of the separated species from the entropy content of the complex for both cases: in the absence and in the presence of the methyl groups on the CD skeleton. Since the difference in the entropy term was below 1 percent, they concluded that the vibrations of methyl groups do not affect the entropy change associated with the formation of the complex. Therefore, in this work the RAMEB was considered as negatively charged species of the native BCD. All the geometry optimizations were carried out using semiempirical methods at AM1 level of theory using Fletcher – Reeves conjugate gradient method with 0.01 kJ/mole convergence criteria.

All of the calculations were performed by the methods described above implemented in the HyperChem code.

### 3.3.2 Determination of the thermodynamic parameters of the SMT-BCD or SMT-RAMEB complexes

In order to determine the thermodynamic parameters of SMT- BCD or SMT-RAMEB complexes at 298.2 K, the enthalpy change and the entropy change are considered in the common way as follows (Eq.1 and 2):

$$\Delta H_{\text{complexation}} = H_{\text{SMT-BCDs}} - (H_{\text{free SMT}} + H_{\text{free BCDs}}) \quad (1)$$

$$\Delta S_{\text{complexation}} = S_{\text{SMT-BCDs}} - (S_{\text{free SMT}} + S_{\text{free BCDs}}) \quad (2)$$

Boltzmann statistics was applied to determine the entropy terms of the species interacted. The vibrational motions give the larger contribution to the entropy. Accordingly, after the vibrational frequencies were calculated in harmonic approximation, the entropy was determined as follows (Eq.3):

$$S_{\text{vib}} = R \sum_i \left\{ \frac{hv_i/KT}{e^{(hv_i/KT)} - 1} - \ln[1 - e^{(hv_i/KT)}] \right\} \quad (3)$$

Where the  $\nu_i$  is the frequency of vibration and  $T$  is the temperature (298.16 K). Geometry optimizations have been calculated by semi-empirical MINDO/3 level

using HyperChem 8 code. After the total energies of the species interacted determined by MINDO/3 level, the vibrational-rotational analysis was performed in harmonic approximation using AM1 approximation.

Neutral aqueous environment was considered by the TIP3P solvation model implemented in HyperChem code [121]. The TIP3P solvation model considers the solvent molecules explicitly, i.e. individual solvent molecules are presented in the simulated system and direct interactions of solute-solvent and solvent-solvent molecules are considered. This model was developed originally for water and extended later to other solvents. The different explicit solvation models, so as this TIP3P model, have their own parametrization, which predicts the physical properties of the liquid during the calculations. Comparing with continuum models, where the solvent molecules are considered as a continuous medium and the solvent are represented usually by its dielectric constant and volume, TIP3P explicitly considers the solvent molecules. This property offers the chance to consider the microsolvation, i.e. consideration the interactions raises by the coordination of individual solvent molecules to the solutes interacted. Therefore, the explicit solvation models are combined with molecular mechanics, molecular dynamic or semi-empirical calculations. Considering the huge computational requirements of the explicit solvent models, in our present case, semi-empirical methods (AM1 and MINDO/3) have been used for the molecular modeling calculations. First the host, guest and host-guest complexes were optimized in vacuum, then these structures were placed into a 30 Å x 30 Å x 30 Å sized cube (Figure 9). The cube was filled with explicit water molecules. The number of the solvent molecules determined the algorithm of the TIP3P solvation model implemented in HyperChem code. After that, molecular dynamic simulation was done for 10 ps at room temperature using MM+ forcefield to reach the system close to the equilibrium. From this equilibrated system further calculations in the presence of explicit water molecules for the complexes and the separated species interacted were performed at MINDO/3 level. Solvent density is also ensured by this model during the simulations because when one solvent molecule exits on one side of the cube, another one enters into the cube at the opposite side. One more reason why we have chosen this model is, that it is possible to mimic the ionic strength of the aqueous buffer by replacing some water

molecules by the ionic components of the applied buffer. In our present case  $\text{HPO}_4^{2-}$ ,  $\text{PO}_4^{3-}$ ,  $\text{K}^+$ ,  $\text{Na}^+$  and  $\text{H}_3\text{O}^+$  ions were considered according to the composition of the phosphoric buffer solution at pH 7, 5 and 2.

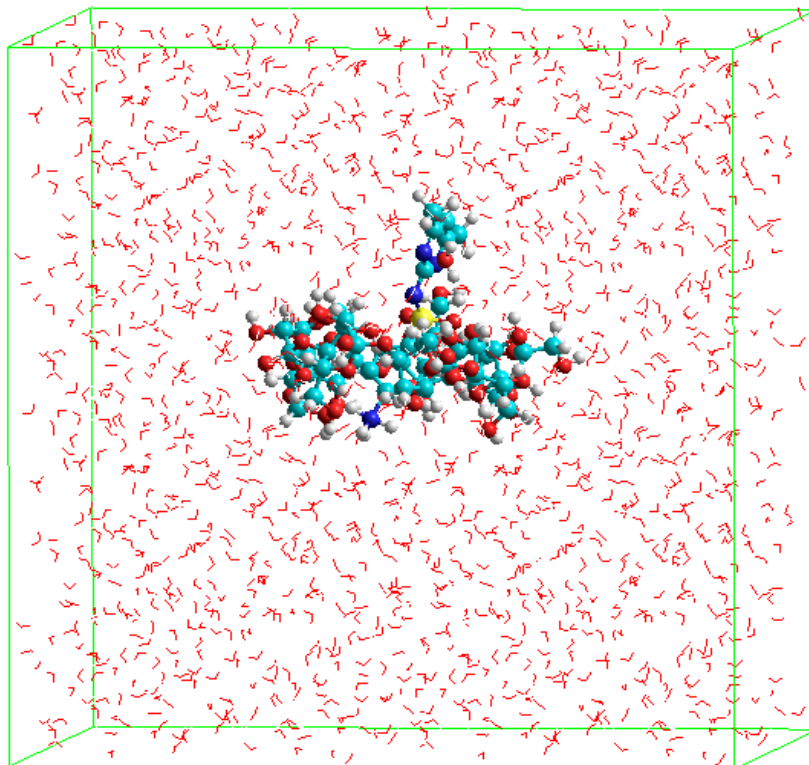


**Figure 9** SMT-BCD complex in the 30 Å x 30 Å x 30 Å sized cube filled with water



# Chapter 4

---

## 4 Results and discussions

### 4.1 The protonation states of SMT molecule

SAs structure contains one basic amine group ( $-\text{NH}_2$ ) and one acidic amide group ( $-\text{NH}-$ ) which resemble  $\text{p}K_{\text{a}1}$  and  $\text{p}K_{\text{a}2}$ , respectively. Theoretically, two possible protonation routes can be considered:

1. Neutral, monoanionic and dianionic
2. Cationic, nonionic, zwitterionic and anionic

From the theoretical point of view both series can be stable in vacuo, while only the second route is stable in aqueous phase. Therefore, the molecular environment affects the preference within the two routes. Especially, in aqueous phase the amine group has the capacity to accept a proton while amide group can release a proton under specific pH conditions. SMT has the  $\text{p}K_{\text{a}1} = 2.07$  (related to the aromatic amine) and the  $\text{p}K_{\text{a}2} = 7.49$  (related to the sulfonamide nitrogen) [68], although these values vary slightly with the analysis used, e.g.  $\text{p}K_{\text{a}1} = 2.65$  [122] or  $\text{p}K_{\text{a}2} = 7.65$  [123] also has been reported. Based on the first data pair the protonation state for SMT has been calculated using HySS2009 program [124], to get the species' concentrations before the investigation. Figure 10 shows the percentage amount of SMT of the three different species via pH, namely cationic, nonionic and anionic. It can be clearly seen that at pH 2 cationic and nonionic, at pH 5 only nonionic, at pH 7 nonionic and anionic, while at pH 10 only anionic form are available in aqueous solutions.

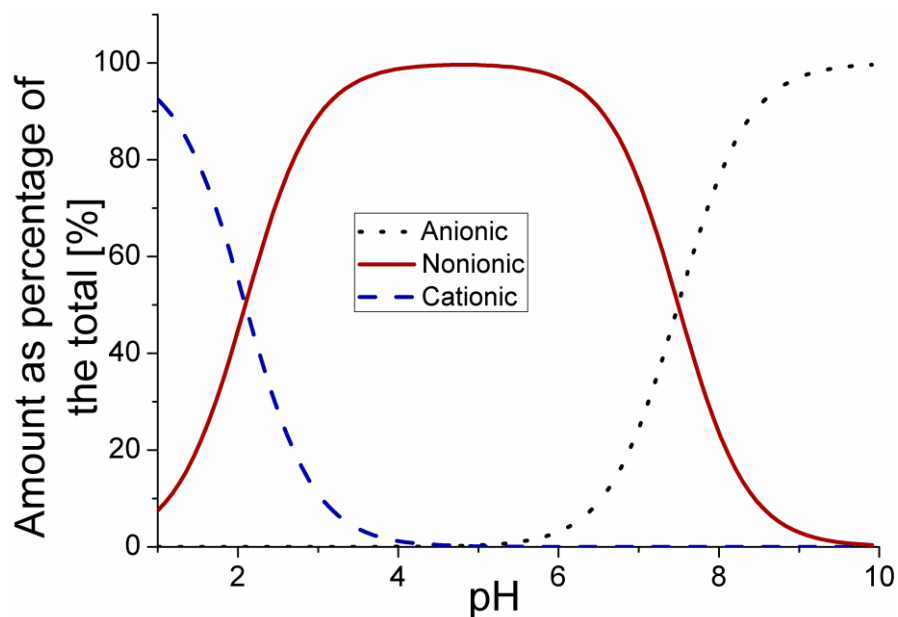


**Figure 10** Distribution diagram of  $\text{SMT}^+$ ,  $\text{SMT}^0$  and  $\text{SMT}^-$  species as a function of the pH

#### 4.1.1 Optical spectroscopic properties of SMT

The optical spectroscopic properties of the pure SMT in phosphate buffer have been investigated first. UV-VIS absorption spectra of pure SMT at four different pH are plotted in Figure 11.

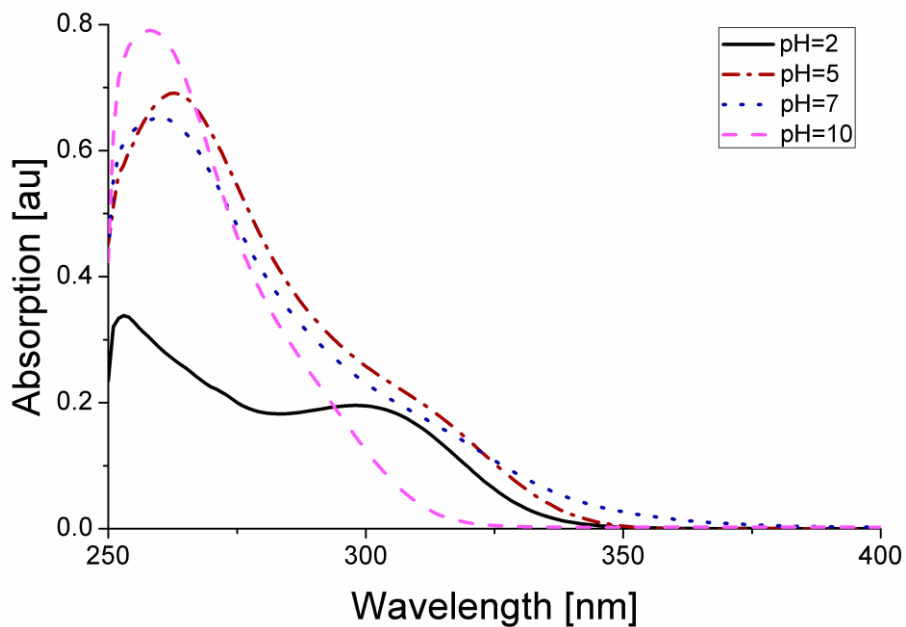


**Figure 11** Absorption spectra of pure SMT at pH 2, 5, 7 and 10

Obviously, the different forms of SMT show different absorption properties and spectral changes are in good agreement with the known acid dissociation constant. Two characteristic peaks can be obtained at about 280 nm and 310 nm. In agreement with the literature, according to the absorption behavior of sulfamethizole [1], the increase of the peak at 280 nm or decreasing the peak at 310 nm reflect the deprotonation of the  $-NH_2$  or  $-NH-$  groups upon elevating the pH, respectively. The fluorescence spectral properties of SMT in different buffer solutions have also been investigated by recording the PL emission spectra. Using 280 nm as excitation wavelength, pure SMT showed two emission maxima, (Figure 12): at pH 2, the emission maxima were observed at 340 and 400 nm, while the strong large peak at 400 nm disappeared with the elevation of pH. Because of this latter peak is significantly lower and missing above pH 5, presumably, it belongs to the cationic form of the drug. The weaker peak at the shorter wavelength remains nearly unchanged in all samples containing nonionic and/or anionic SMT.

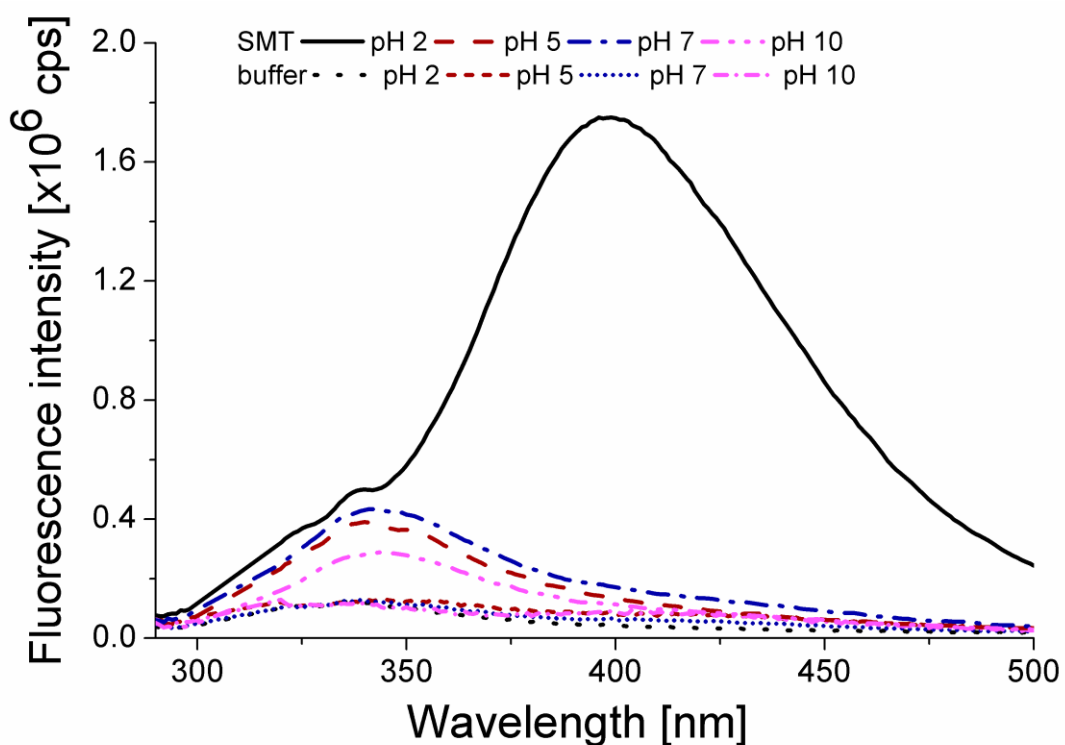


**Figure 12** Emission spectra ( $\lambda_{exc} = 280$  nm) of pure SMT at pH 2, 5, 7 and 10

### 4.1.2 Protonation states and structures of SMT molecule

The energetically favorable deprotonation route of SMT molecule was determined at molecular level using molecular modeling calculations. Along with the known forms, i.e. cationic ( $\text{SMT}^+$ ), anionic ( $\text{SMT}^-$ ) and nonionic ( $\text{SMT}^0$ ), the presence of zwitterionic form ( $\text{SMT}^\pm$ ) of this drug stabilized on adsorbed state has also been reported [104]. During the calculations the cationic, nonionic, zwitterionic and anionic routes have been considered. Figure 13 shows the two deprotonation steps related to the changing pH from low to high: at low pH the aromatic amine is protonated, therefore the  $\text{SMT}^+$  ion is presented, but when the pH increases from 2 to 5, the ion will lose one proton and SMT will be nonionic i.e.  $\text{SMT}^0$  or/and zwitterionic ( $\text{SMT}^\pm$ ), then in higher pH the sulfonamide nitrogen will lose its proton as a second deprotonation step resulting in the  $\text{SMT}^-$  ion. Therefore, the SMT present at pH 5 as a neutral form which includes nonionic  $\text{SMT}^0$  and zwitterionic  $\text{SMT}^\pm$ .

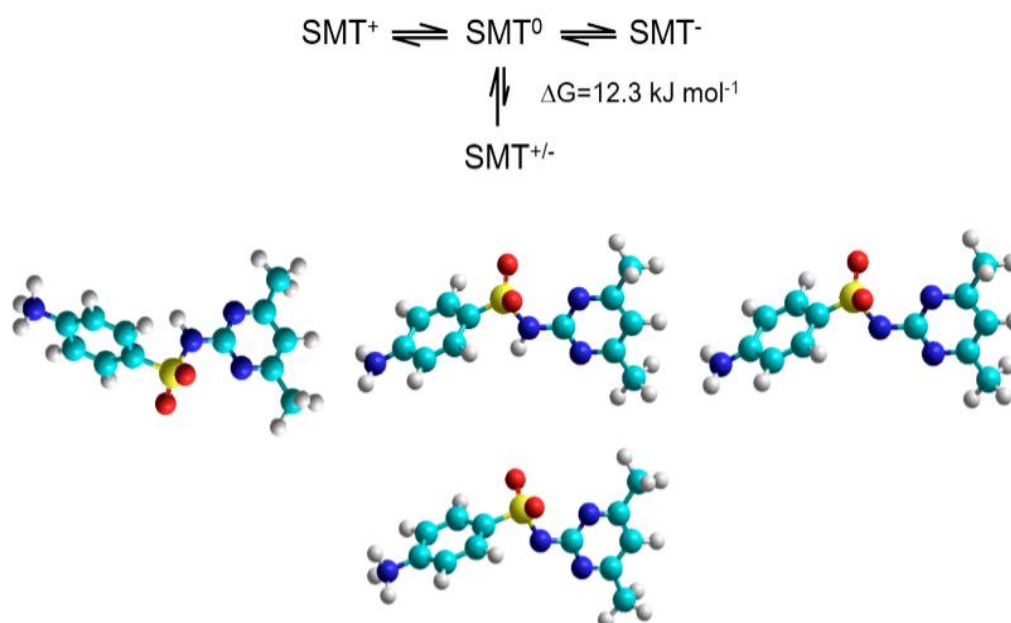


**Figure 13** The energetically most favorable deprotonation routes of SMT (cationic: left, nonionic: middle, anionic: right, zwitterionic: bottom) determined by MINDO/3 approximation using the TIP3P solvation model for the buffer [125]. Gibbs free energy between the nonionic and zwitterionic forms suggest the presence preferably of nonionic form in the solution

From the calculations in aqueous solutions of buffer, the Gibbs free energy difference between the nonionic and zwitterionic forms of SMT was found to be 12.3 kJ mol<sup>-1</sup> in this environment, which is comparable with the experimentally determined value of 15.7 kJ/mol [104]. From the calculated  $\Delta G$  value the estimated amount of SMT<sup>±</sup> is 0.7 %, which confirms the experimental findings of Shakuri and Ishimitsu [126], namely, less than 2 % of SMT exist in the zwitterionic form in aqueous solution. This result suggests the presence of SMT in nonionic rather than zwitterionic form in the aqueous solution phase.

## **4.2 Inclusion complex formation between SMT and CDs**

### **4.2.1 Complexation stabilities of SMT– BCD and SMT-RAMEB at varying pH**

Based on our analyses described above we can conclude that under the applied experimental conditions the SMT are presented in reasonable assume cationic and nonionic, nonionic, nonionic and anionic or anionic forms at pH 2, 5, 7 or 10, respectively. In this way, it is possible to analyze the potential differences or the similarities between the interaction of BCD or RAMEB with cationic, nonionic and anionic forms of SMT. First, the spectral changes in the absence and presence of BCD or RAMEB (0–3 mM) were investigated. From Figure 14 a) and b), it is clear that under acidic circumstances, the emission maxima of SMT appearing approximately at 340 and 400 nm increased in the presence of CDs and no significant red or blue shift in the emission spectrum of SMT was observed. For the later determination of the association constant (see below) related to the complex formation, both 340 and 400 nm have been selected. With the elevation of the pH only one noticeable emission peak at 340 nm could be detected (Figure 14 c), d) e), f), g) and h)) and this peak also increased in the presence of CDs.

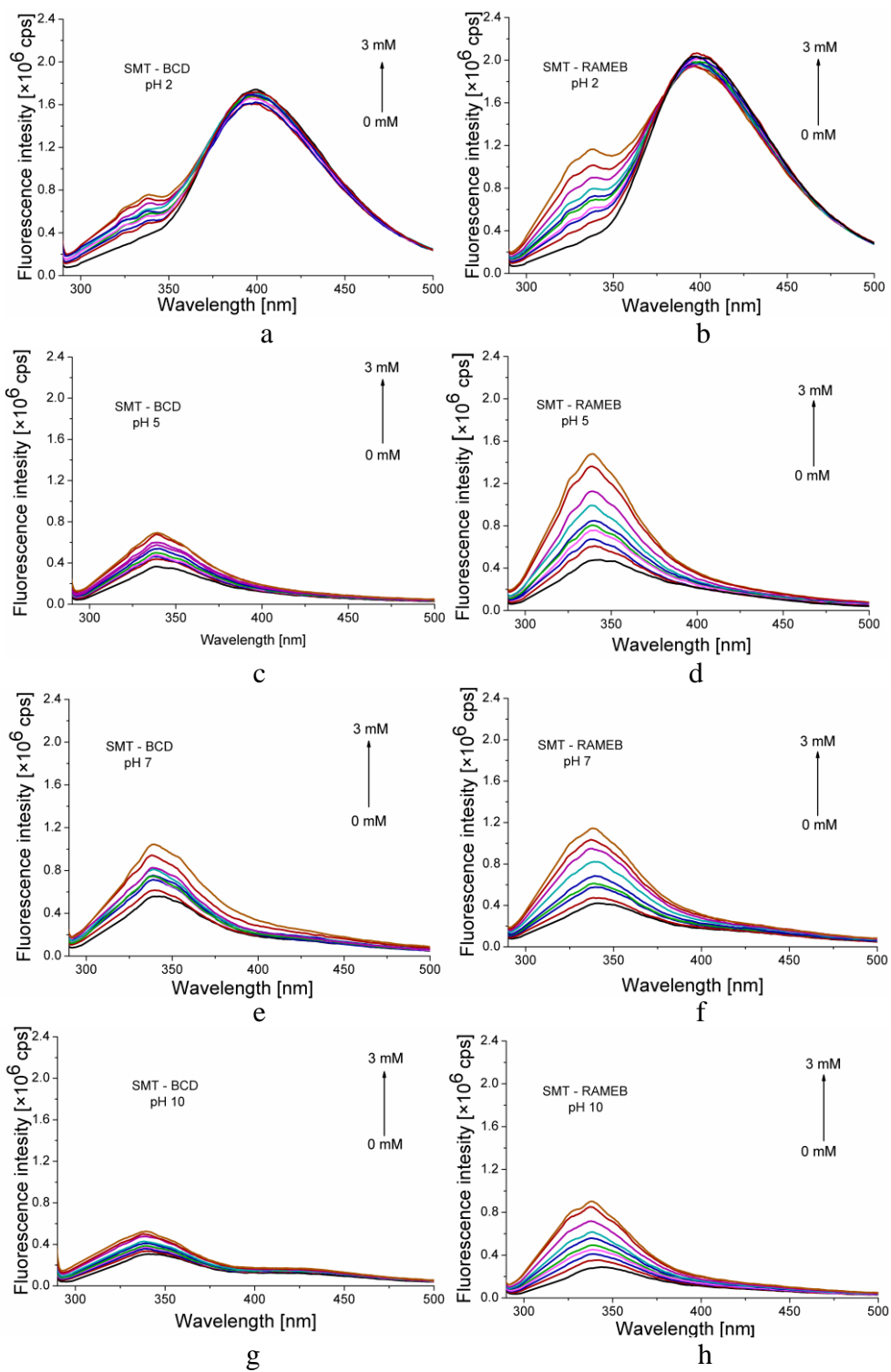


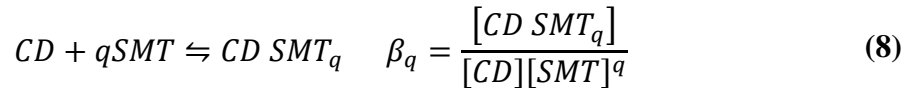
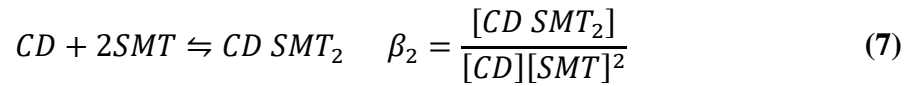
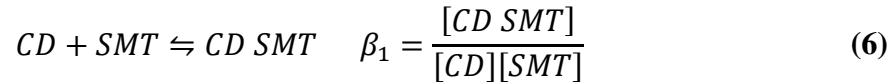
**Figure 14** Fluorescence emission spectra of SMT in the absence and presence of increasing BCD (a, c, e, g) and RAMEB (b, d, f, h) at pH 2, 5, 7 and 10 ( $\lambda_{exc}=280$  nm)

Similarly to our previous studies [127,128], a non-linear fitting method was used to calculate the association constants of the complex formation based on the fluorescence emission data for all the experiments performed with the HyperQuad2006 program package [129]. The following equations are implemented in the program code:



$$\beta_{pq} = \frac{[CD_pSMT_q]}{[CD]^p[SMT]^q} \quad (5)$$

Where p and q are the coefficients that indicate the stoichiometry associated with the possible equilibrium in the solution. Furthermore, all equilibrium constants are defined as overall association constants:



The relationship between the overall association constants  $\beta_i$  and the stepwise association constants  $K_i$  is:

$$\beta_1 = K_1; \beta_2 = K_1 \times K_2; \beta_q = K_1 \times K_2 \dots \times K_q \quad (9)$$

From the model of the lowest standard deviation, the stoichiometry and association constants of the complex formation process were determined by data evaluation.

The logarithm of the association constants ( $\log K$ ) related to the complex formation between SMT and BCD or RAMEB at pH 2, 5, 7 and 10 were determined as shown in

Table 1. The data are small ( $\log K \sim 3$ ) and indicate weak but relevant interaction between the species applied. Furthermore, our earlier works [108,89] showed that guest molecules with similar size like SMT form a more stable complex with RAMEB than BCD does because in both directions the extended cavity of BCD by the methyl groups could offer a more complete and deeper penetration of the guest molecule inside the methylated BCD. Surprisingly, in the present case, the stabilities of the investigated CDs' complexes of SMT were independent from the BCD derivatives. Accordingly, due to the association constant values (Table 1), it seems that the process is more sensitive for the ionic form of SMT than the functionalization of the CDs. Although significant difference only between the association constants at pH 2 and at higher pH has been found, these data are indicating that the cationic species of SMT form weaker complex with BCD and RAMEB than nonionic and anionic SMT molecules.

**Table 1** Stabilities ( $\log K \pm \text{SEM}$ ) of SMT-BCD complexes (the unit of  $K$  is  $\text{dm}^3/\text{mol}$ )

<b>pH</b>	<b>SMT-RAMEB</b>	<b>SMT-BCD</b>
2.0	2.1 <sup>a</sup> ±0.1	2.0 <sup>a</sup> ±0.2
5.0	3.1 <sup>b</sup> ±0.1	2.9 <sup>b</sup> ±0.3
7.0	3.0 <sup>b</sup> ±0.2	3.0 <sup>b</sup> ±0.2
10.0	3.1 <sup>b</sup> ±0.1	2.9 <sup>b</sup> ±0.4

<sup>a,b</sup> Means followed by the same letter are not significantly different ( $p < 0.01$ ).

#### **4.2.2 The possible structures of SMT- BCD and SMT- RAMEB complexes**

Taking into account the three forms ( $\text{SMT}^+$ ,  $\text{SMT}^0$ ,  $\text{SMT}^-$ ) presented in the applied solution phase the most important task was to determine their complexations with BCD and RAMEB host molecules in the aqueous buffers at molecular level. The



computational procedure for a big system is very long, therefore the system was modified considering the slightly negatively charged cavity of RAMEB molecules by the negatively charged parent BCD (see details in Chapter 3.3.2). Obviously, it is reasonable to assume that the electron rich cavity of the parent BCD itself and the negatively charged RAMEB cavity result in repulsive Coulomb interaction between the CD host and the anionic SMT guest, which repulsion will reduce the secondary interactions between the host and guest molecules. However, the interaction between SMT<sup>-</sup> and the host molecules are stronger and more stable than the interaction with the other SMT ionic forms. Analyzing the theoretically determinate structures (Figure 15) it can be explained as follows: at low pH the cationic SMT molecule enters into the host cavity with its aromatic amine moiety, while at higher pH with its methyl substituents. In the former cases, hydrogen bridges between the (guest amine) N-H ... O (host hydroxyl) which are responsible for the stabilization of the cationic SMT form, while in the latter cases, the hydrogen bridges between the (guest methyl) C-H ... O (host hydroxyl) moderate the weak interactions between the host and guest. In this way, it can be concluded that electrostatic forces are responsible for these unexpected results which orient SMT compound before penetrating inside the BCD cavity. Additionally, this pH dependent orientation of the guest molecule in the complexes can explain the earlier contradictory description of the SMT-CD structures. Those results are based on combined NMR and molecular modeling results and described the complex structure as the inclusion of the aniline moiety [1], or the inclusion of the pyrimidine ring [90] through the CD cavity was found.

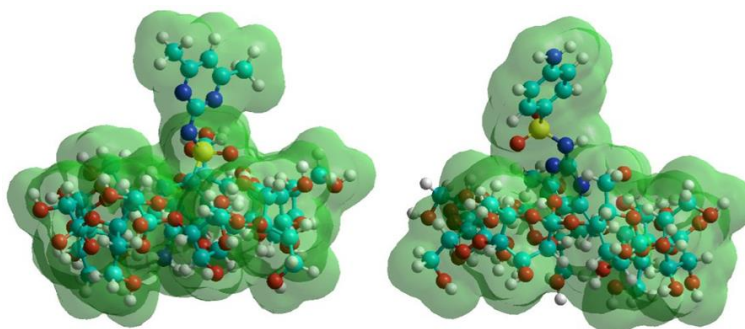


**Figure 15** Equilibrium conformation of SMT-BCD complexes. a) SMT molecules with their aromatic amine moiety and b) with their methyl groups enter into the cavities of hosts

### 4.2.3 Thermodynamic studies

Temperature dependent PL measurements have been done with the aim to study how the association constant of the complex formation between SMT and BCD or RAMEB depends on the temperature at different pH. The logarithm of the association constant at four different temperatures between 298.2 and 313.2 K are summarized in Figure 16. Although the association constants of CDs' complexes generally decrease with the elevation of the temperature [130], our earlier work [89] shows an example for the opposite tendency. In the present case with the elevation of the temperature the complex stability increased and decreased at pH 2 and 7, respectively. This means that the presence of SMT<sup>+</sup> at pH 2 and SMT<sup>-</sup> at pH 7 contrary affects the stability of the complex. At pH 5 only the neutral form of the guest are in a considerable amount, and the association constants at room temperature related to the SMT – CD complexes show no significant changes in the functionalization of the BCD molecule by methyl groups (log  $K = 2.9$  vs. log  $K = 3.1$ ). Therefore, it is surprising that at pH 5 the substitution of the BCD affected the dependence of the complex stabilities on the temperature.

Due to the weak interactions between the molecules, the dependence of complex stabilities on the temperature is slight and indicates that the enthalpy change is low. To get more information about the related process, the thermodynamic parameters have also been determined using the van't Hoff plot (Figure 16) and applying the van't Hoff equation (Eq. 10):

$$\ln K = -\frac{\Delta G}{RT} = -\frac{\Delta H}{RT} + \frac{\Delta S}{R} \quad (10)$$

$\Delta H$  and  $\Delta S$  are the enthalpy and entropy changes of the complex formation, and  $\Delta G$  is the Gibbs free energy change.  $R$  stands for the gas constant, while  $T$  is the temperature in Kelvin.

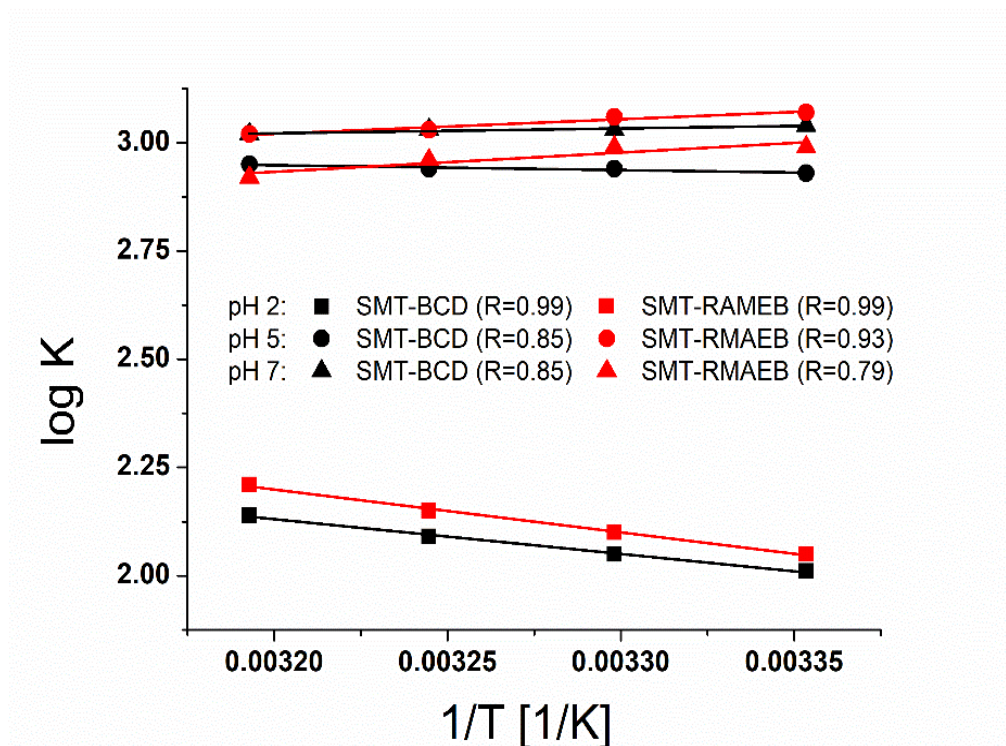


**Figure 16** van't Hoff plots of complex formation between SMT and BCD or RAMEB at pH 2, 5 and 7

**Table 2** Thermodynamic parameters associated to the formation of SMT-CD complexes. Data are determinate based on temperature-dependent fluorescence spectroscopic measurements. ( $\Delta H$  [kJ mol<sup>-1</sup>],  $\Delta S$  [J K<sup>-1</sup> mol<sup>-1</sup>],  $\Delta G_{298\text{ K}}$  [kJ mol<sup>-1</sup>])  $\pm$ SEM

Host species	pH	$\Delta H$	$\Delta S$	$\Delta G_{298\text{ K}}$
<b>BCD</b>	2	15.4 $\pm$ 0.8	90.0 $\pm$ 2.5	-11.4 $\pm$ 1.5
<b>RAMEB</b>		18.9 $\pm$ 0.8	102.7 $\pm$ 2.6	-11.7 $\pm$ 1.6
<b>BCD</b>	5	2.2 $\pm$ 0.5	63.3 $\pm$ 1.7	-16.7 $\pm$ 1.0
<b>RAMEB</b>		-6.4 $\pm$ 1.0	37.2 $\pm$ 3.3	-17.5 $\pm$ 2.0
<b>BCD</b>	7	-2.2 $\pm$ 0.5	51.0 $\pm$ 1.7	-17.3 $\pm$ 1.0
<b>RAMEB</b>		-8.5 $\pm$ 1.2	28.8 $\pm$ 3.8	-17.1 $\pm$ 2.3

Thermodynamic parameters are summarized in Table 2. The complex formations of SMT with BCDs were spontaneous, because of the negative  $\Delta G$  values. At pH 7 results show that association was exothermic, while at low pH (pH = 2) endothermic molecular association was obtained. Furthermore, at pH 5, the methyl group of BCDs changed the endothermic character of the complex formation to exothermic. Furthermore, positive entropy change was observed for each complex formation, however, it was compensated by the enthalpy change. The solvation shell released when the SMT molecule entered the CD cavity and this probably caused the entropy increase during the association reaction. Moreover, the removal of more or less water molecules from the solvation shell regarding the molecules interacted during the formation of complexes, thus, higher entropy. When the pH is high, the entropy changes decreased, which may be related to lower releasing water molecules from the solvation shell of SMT molecules, because the stabilization is also supported by the attractive Coulomb forces between the negatively charged SMT and the dipole moments of the solvent molecules. The correlation between the enthalpy and the entropy changes can be explained by the changes of the solvation shell of guests, since the removal of less water molecules from the solvation shell requires less energy. This description agrees with the enthalpy-entropy compensation and highlights that the exothermicity of molecular association usually restricts the movement of the constituents, thereby causing increasing entropy loss.

**Table 3** Thermodynamic parameters associated to the formation of SMT-CD complexes. Semiempirical MINDO/3 method with TIP3P solvation model is applied. ( $\Delta H$  [kJ mol<sup>-1</sup>],  $\Delta S$  [J K<sup>-1</sup> mol<sup>-1</sup>])

host species	host simulated as	guest's charges							
		+1 (cationic)		0 (nonionic)		0 (zwitterionic)		-1 (anionic)	
		$\Delta H$	$\Delta S$	$\Delta H$	$\Delta S$	$\Delta H$	$\Delta S$	$\Delta H$	$\Delta S$
BCD	0 BCD	16.3	93.0	9.3	78.2	5.4	68.4	-3.7	47.5
RAMEB	-1 BCD	19.1	105.4	14.3	99.7	-8.7	35.2	-9.4	26.4

In order to interpret the BCD functionalization dependent opposite enthalpy change at pH 5, the thermodynamic parameters of the complex formation have been determined using molecular modeling methods. These theoretically calculated thermodynamic parameters (Table 3) are in good agreement with the experimental data (Table 2). It is clear that all entropy data of the interactions are positive, but the entropy value decreased for the anionic form of SMT with CD. This result may be due to three causes: 1. SMT molecules totally or at least partly lose their hydration shell. 2. It is expected to remove the solvent water molecules from the host's cavity before the complex formation. Both causes increased entropy. 3. Probably the presence of hydration shell surrounding the anionic SMT is more stable, therefore the entropy gain decreases for the anionic SMT form with CDs interactions. The dehydration process leads to combining the SMT and part of the CD by hydrogen bond formation. Dehydration requires energy, but this energy is compensated by the entropy arising from the increasing freedom of the water molecules after the dehydration. This description is supported by the good agreement between the measured and calculated thermodynamic parameters.

Obviously, during the calculation of SMT-CD complex structures, we found that in the case of RAMEB, the formation of the zwitterionic form of SMT is significant. When the guest molecule enters with its aromatic amine moiety into the RAMEB cavity, the proton is transferred from the sulfonamide to the amine moiety. This tautomerization of SMT enhanced by the Coulomb interaction of the proton with the negatively charged cavity of the host. This finding can explain the experimentally found negative enthalpy change related to SMT–RAMEB complex formation at pH 5. To justify this theoretically found conception, simultaneous analysis of the complexation behavior was carried out using FT-IR spectroscopy.

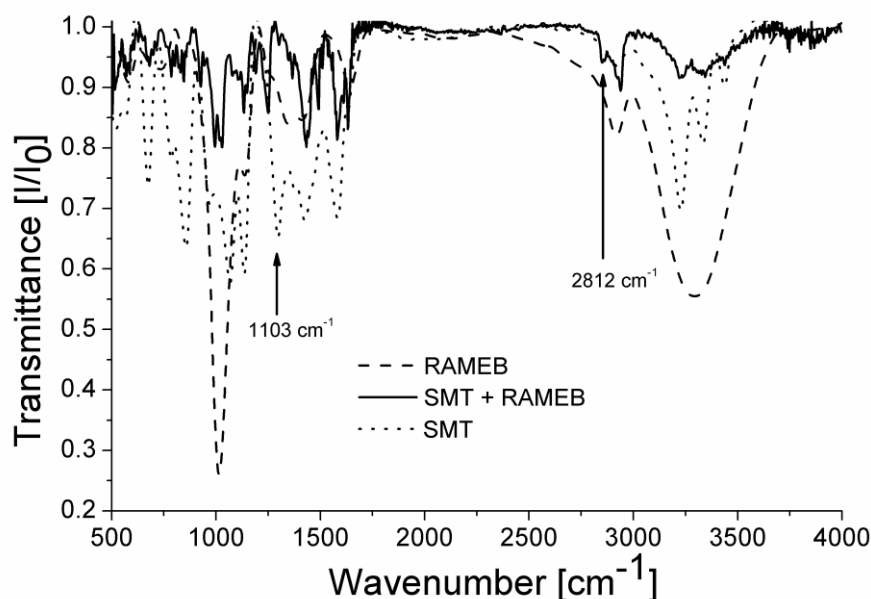


**Figure 17** Infrared spectra of SMT-RAMEB complexes

As expected, our results are in agreement with the IR analyses of SMT-BCD complexes prepared by Zoppi *et al.* using freeze-drying method [78]. In good agreement with our results they also found that the characteristic bands of SMT shifted and are more or less intense in the presence of BCD. FT-IR spectra of the SMT-RAMEB complexes and the interacting species gave additional information on the complexation process and support our idea described above. Figure 17 shows that significant changes of two characteristic vibrations of SMT molecules were observed due to the complexation with RAMEB host as follows: the belting vibration of SNH bond angle at  $1103\text{ cm}^{-1}$  which is related to sulfonamide moiety disappeared, at the same time the bond stretching, which is related to the aromatic  $\text{-NH}_3^+$  appeared at  $2812\text{ cm}^{-1}$ . These changes are regarding the stabilization of the zwitterionic form of SMT in the RAMEB cavity. This behavior has been observed in the case of the RAMEB but has not been found in the spectra related to the complexes of BCD host. This information is in agreement with our experimental result and supports the theoretical findings of  $\text{SMT}^\pm$ -RAMEB complexes.

#### 4.2.4 Driving forces of the complex formation SMT and BCDs

The thermodynamic parameters derived from temperature-dependent spectroscopic measurements are constant in the temperatures range (298.2–313.2 K). Furthermore,

these data reflected the way how the association constants have been determined and the temperature-dependent change of the association constants values. Due to the choice of the spectroscopic method for investigation the stabilities of the complexes and depending on the environmental conditions, it is important to study the details of the environment around the guest when the molecule enters from the polar aqueous media into the hydrophobic cavity of the CD, thus, the related enthalpy changes and entropy change explains the complex formation without solvent interaction in the bulk phase. In this work, the fluorescence spectroscopic measurements and van't Hoff equation have been applied to determine the thermodynamic parameters. Isothermal titration calorimetry (ITC) is the accurate technique for directly measuring thermodynamic properties of host-guest complex formation, however relevant experiments showed [87] that in the case of CDs' complexes the thermodynamic parameters derived from spectroscopic data or measured directly with ITC are almost similar and the difference between the two methods is slight. Therefore, the following interpretation of our data is relevant.

The possible mechanisms, which are acting as driving forces and are responsible for the stabilities of the host-guest complexes of CDs, include [25]:

- Electrostatic interaction,
- hydrophobic interaction,
- van der Waals interaction,
- hydrogen bonding,
- charge transfer interaction and
- removal of the water molecules from the hydrophobic cavity of the CDs to the bulk phase.

Thermodynamic parameters explain the contribution of the SMT species' desolvation and various types of noncovalent interactions listed above. In fact, van der Waals force and hydrogen bonding or hydrophobic interaction in the complex formation play a role for both negative and positive enthalpy and entropy changes, respectively. On the other hand, electrostatic driving forces combined with hydrogen bonds of ionized groups are responsible for the higher negative values of  $\Delta H$  combined with positive  $\Delta S$  [131]. It is important to study the tendencies observed in

the thermodynamic parameters, losing the proton of SMT ions which change the ionic form in the order  $\text{SMT}^+$ ,  $\text{SMT}^0$ ,  $\text{SMT}^-$ , and this change leads to a decrease of enthalpy and entropy. According to this principle, taking into account the attractive forces between the anionic cavity of the host and the cationic guest at pH 2, highly negative enthalpy changes should be observed in vacuo, but the guest desolvation needs energy more than it produces during the association of SMT with the CD, so positive enthalpy changes can be observed. Furthermore, the increase in the entropy returns to break down of the solvent molecules in the solvation shell, thus these molecules become free and increase the entropy. At pH 5, the neutral form of SMT is available. Due to the low solvation shell stability, then much less energy is needed for destroying the shell, consequently, the enthalpy change of the complexation is lowered rather than the weaker contribution of the attractive Coulomb forces. Moreover, the same effect on the entropy is present, i.e. the lower stability of the solvent molecules in the solvation shell surrounding the guest assumes higher entropy content of the solvent molecules prior to complex formation which property causes lower entropy gain during the interaction with the CD hosts. At pH 5, zwitterionic form of SMT is presented in a special case, i.e.  $\text{SMT}^{\pm}$ - RAMEB complex. The presence of  $\text{SMT}^{\pm}$  affects the complex formation however, and this probably enhances the decrease of the enthalpy when the positively charged  $-\text{NH}_3^+$  group of SMT interact with the highly negatively charged cavity of the RAMEB while the negative sulfonamide nitrogen of SMT interacts with the positively charged methyl groups of the host. Overall, at pH 5 the competition will be between three effects (Coulomb interaction, desolvation of the guest prior formation of the complex and the formation of zwitterionic derivative of the SMT). At pH=7 two forms of SMT, neutral and anionic are present in aqueous solution. The complex formation explains the complex stabilization effect of the deprotonated SMT nitrogen on the additional decreasing of the two enthalpy and entropy changes. Furthermore, to gain details of the competition effects of the complexation processes above, enthalpy – entropy compensation has been analyzed. The enthalpy-entropy compensation exhibits a linear relationship between thermodynamic parameters. This compensation attracts scientists' attention as it is an unresolved phenomenon in chemical thermodynamics [132,133]. Figure 18 shows the  $\Delta H$  vs.  $\Delta S$  plot for SMT-



CD complexes analyzed in the present work. The plot includes the experimentally and the theoretically determined data. The temperature range of the measurement investigated is small (298.2-313.2 K), but the compensation temperature determined from the slope of the good straight line (387 K and 374 K experimental and theoretical data, respectively) are far from the average temperature. This small difference could arise from the indirect determination of the thermodynamic parameters based on spectroscopic measurements. Furthermore, the difference between the  $\Delta G$  values ( $\sim 6.1$  kJ mol<sup>-1</sup> in the present systems) brings the experimental and compensation temperature farther [134].

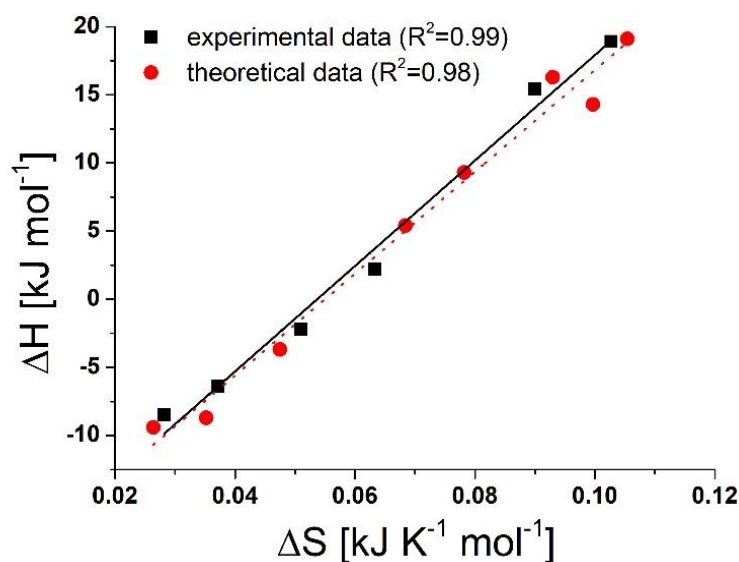


**Figure 18** Enthalpy-entropy compensation plot of SMT- BCD and SMT-RAMEB complexes

The compensation effect refers to the behavior of a series of closely related chemical reactions. Obviously, in the supramolecular chemistry systems, especially in CD molecules, the enthalpy-entropy compensation was investigated 20 years ago and more than 1000 thermodynamic values of the inclusion complexes of native and chemically-modified CDs were studied [21]. Depending on the studies of the enthalpy-entropy compensation plot of native and modified CDs or the  $\alpha$ -,  $\beta$ - and  $\gamma$ -CDs, it was found that the linear relationship and the slope of the straight line could be affected by the variance between the conformational change of the native and

modified CDs caused by the desolvation of both CDs and guest molecules, and by the ring size and flexibility. In previous works [25,132], the compensation consequence is mostly interrupted by the changes in the level of hydration and restructuring of the solvent molecules. The significant effect of the solvent is not new, since solvation is recognized to affect the electronic structure of molecules and then affects the interactions between electrons of different atomic or molecular orbitals, accordingly, it also affects the molecular interactions, particularly when they are weak [135,136]. In our present study, if the anionic SMT form molecule keeps the part of its solvation shell, then the higher ordered structure of the complexes (included by its solvation shell) explains the deprotonation enhanced gain entropy decreases. Because there is no significant difference or clear difference, it is difficult to distinguish between the cavity size and elasticity of BCD and RAMEB and the richness of the enhanced electron-enhanced aspect of the methylated CD will have an adverse effect on the results that have emerged, and we can explain the differences in the small entropy term by the weak solubility of the BCD. (Because there is highly arranged water molecules in their melt shell) [14]. As it is known, when guest particles enter the CD cavity, the reaction (at least in part) greatly affects the solvent cortex of the host and may result in a weakening of the CD solvent molecule. This is similar to our previous findings [89], when the solvent molecules leave the host's cavity, reorganization of the more ordered BCD-water structure results in a higher entropy change vs. the less ordered RAMEB-water system.

### **4.3 SMT removal from aqueous solutions by water**

#### **insoluble nanomaterials**

SAs have been found in water, which originate from human and animal waste. Therefore, it is necessary to use some effective substances that have the ability to remove these pollutants by adsorption on their surface. For this purpose, we studied the SMT adsorption onto the surface of BBP and CNTs by applying adsorption isotherm models.

### 4.3.1 Adsorption behavior and mechanisms

The adsorption of drugs on the nanomaterial surfaces commonly determined using one or combination of the following methods:

#### 1- Adsorption isotherms

Adsorption isotherm is the graph between the amounts of adsorbate (x) adsorbed on the surface of adsorbent (m) and the pressure at constant temperature. The isotherm model describes the calculation of the theoretical adsorptive capacity which is the most important indicator for evaluating the adsorbent. The Langmuir, Freundlich, Redlich-Peterson, Temkin, and Dubinin-Radushkevich models are used to describe the adsorption behavior of drugs on nanomaterials [137- 139].

#### 2- Adsorption kinetics

Essential information on kinetic mechanisms can be given by kinetic models to describe the conversion during biomass gasification, which is crucial in designing, evaluating, and improving gasifiers [140]. Kinetic models are accurate and detailed, but also computationally intensive. In general, pseudo-first order, pseudo-second order, Elovich, and intraparticle diffusion models give precise fitting of the adsorption kinetics of aqueous moved by carbon based nanomaterials [141, 142].

#### 3- Adsorption thermodynamics

Thermodynamic equilibrium models, such as models of chemical reaction equilibrium, are regarded to the minimization of the Gibbs free energy of the system. The adsorption thermodynamics of the drugs can be determined by calculating Gibbs free energy, enthalpy change and entropy change [143,144].

In this work the analysis of adsorption isotherms were chosen to describe the possible removal of SMT from aqueous solution using BCD containing polymer or carbon based nanomaterials using Langmuir (Eq.11) and Freundlich (Eq.12) adsorption models:

$$q_0 = (Q_0 \times K_L \times C_e)/(1 + K_L \times C_e) \quad (11)$$

$$q_0 = K_F \times C_e^{(\frac{1}{n})} \quad (12)$$

Where  $q_0$  (mg g<sup>-1</sup>) is the adsorption at the equilibrium,  $Q_0$  (mg g<sup>-1</sup>) is the maximum adsorption capacity,  $C_e$  (mg g<sup>-1</sup>) is the equilibrium concentration in solution,  $K_L$  (L

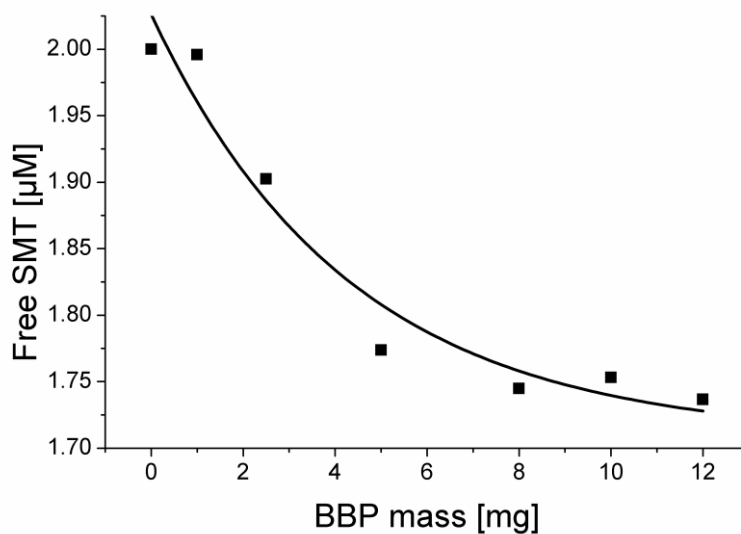
$\text{mg}^{-1}$ ) is the affinity parameter,  $K_F$  ( $\text{mg g}^{-1} (\text{L mg}^{-1})^{n-1}$ ) is the adsorption coefficient, and  $n$  is the adsorption constant as an indicator of isotherm nonlinearity.

#### 4.3.2 Adsorption of SMT by insoluble BCD bead polymer

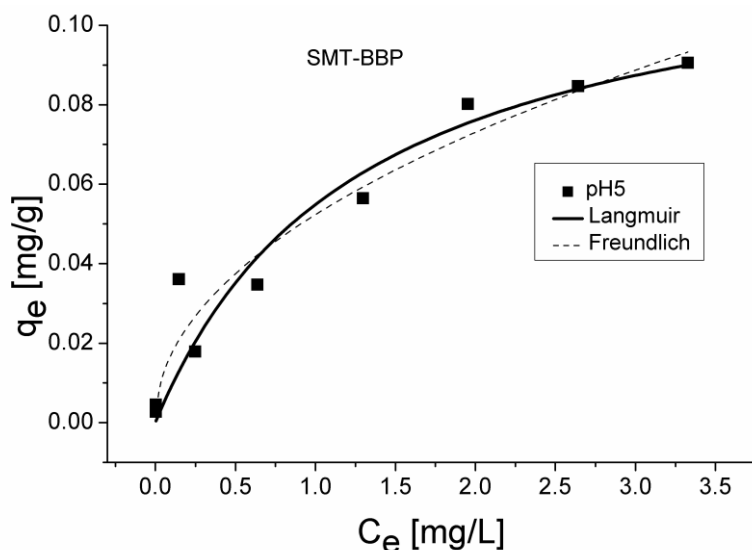
Previous studies demonstrated that based on the formation of stable host-guest complexes, the guest molecule can be effectively removed from aqueous solution using insoluble BCD polymer [see e.g. 41]. However, it is not possible to estimate the adsorption capacity of the polymer based on the association constant related to the BCD-guest complex. Therefore, the efficiency of BBP to remove SMT from aqueous solution has also been tested. In the first step standard amount of SMT was added to increasing amount of BBP at pH 2, 5 and 7. Although Figure 19 a) shows that BBP is removed only a small amount of SMT from aqueous solution, the adsorption isotherms of SMT onto BBP was also tested (Figure 19 b). Table 4 summarize the determinate adsorption isotherm parameters for SMT by BBP at different pH. No preference was found between the Langmuir and Freundlich models with high  $R^2$  values varied in both cases between 0.91 and 0.95. The heterogeneity indexes are close to 1 indicating a relatively homogenous sorption. The maximum quantity of the drug bound per gram of insoluble polymer is the highest at pH 5, however, all of the data are small which indicates that BBP has low efficiency towards SMT under the applied environmental conditions.

**Table 4** Langmuir and Freundlich adsorption isotherm parameters of (SMT) adsorption by BBP at pH 2, 5 and 7.  $Q_0$ ,  $K_L$ ,  $K_F$  and  $n^{-1}$  are  $\pm$  SEM

pH	$Q_0$ ( $\text{mg g}^{-1}$ )	$K_L$ ( $\text{L mg}^{-1}$ )	$R^2$	$K_F$ ( $\text{mg g}^{-1} (\text{Lmg}^{-1})^{(1/n)}$ )	$n^{-1}$	$R^2$
2	$0.1 \pm 0.04$	$0.3 \pm 0.1$	0.969	$0.03 \pm 0.03$	$0.8 \pm 0.1$	0.947
5	$0.1 \pm 0.02$	$0.5 \pm 0.5$	0.988	$0.05 \pm 0.02$	$0.6 \pm 0.1$	0.977
7	$0.1 \pm 0.06$	$0.1 \pm 0.1$	0.964	$0.02 \pm 0.01$	$0.8 \pm 0.1$	0.953



a



b

**Figure 19** HPLC measurement for a) SMT (2  $\mu\text{M}$ ) adsorption on BBP (0-12 mg) and b) adsorption isotherm plot for SMT (0-12.5  $\mu\text{M}$ ) by BBP (2.5 mg) at pH 5

### 4.3.3 Adsorption of SMT onto insoluble CNTs

Because of the slight SMT adsorption onto the insoluble BBP, another group of adsorbents is tested to remove SMT from the aqueous solution. CNTs were found to be an effective adsorbent for several inorganic and organic compounds [54,55], therefore, these nanomaterials have been tested to extract SMT from water.

Since we had experience on the spectral properties of SMT, our first idea was to follow the adsorption process using fluorescence measurements. For the purpose of verifying the results obtained from the fluorescence emission method, we measured the compounds with HPLC for comparison and to ensure the accuracy of the results. Obviously, the adsorption of SMT on MWCNTs or H-MWCNTs showed big difference between fluorescence emission and HPLC measurements (Figure 20).

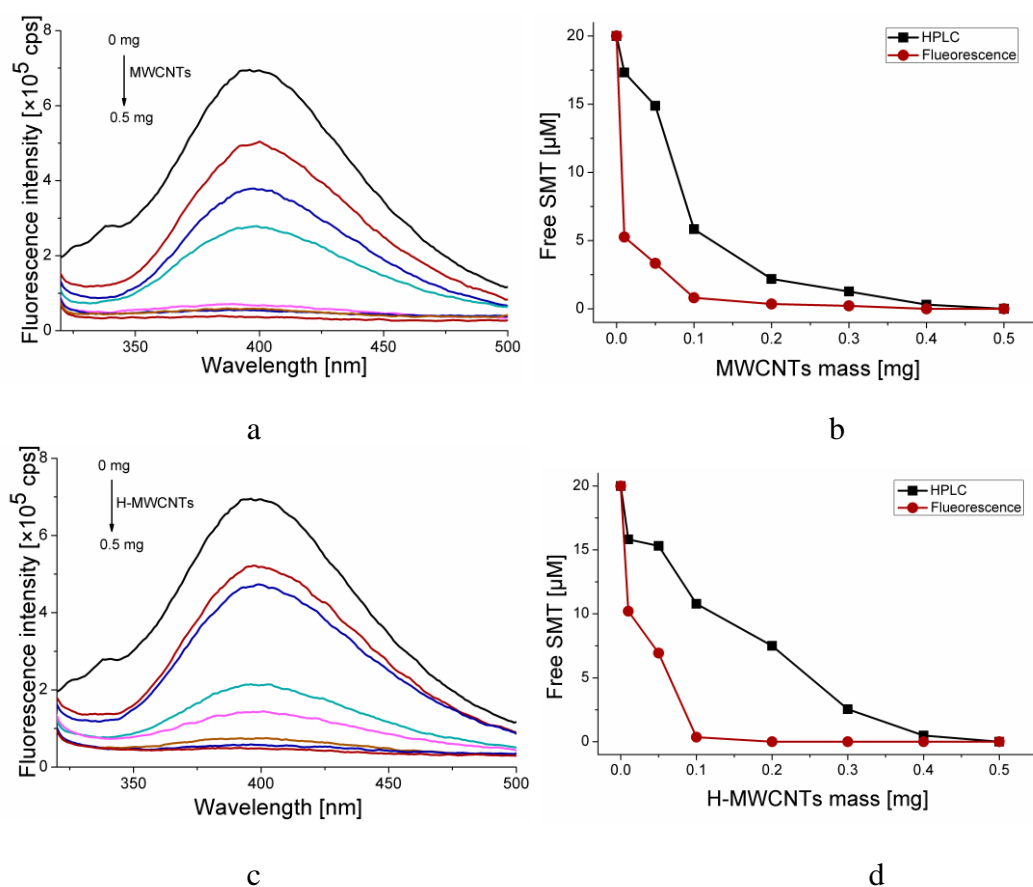


**Figure 20** The fluorescence intensity of the free SMT in the supernatant at pH 2, in the absence or presence a) MWCNTs or c) H-MWCNTs mass (0-0.5mg), Fluorescence and HPLC measurements for SMT (20μM) with b) MWCNTs or d) H-MWCNTs, (0-0.5 mg) interaction at pH 2 and 298.2K

The low intensity of the adsorption observed by fluorescence measurement may be due to the production of the CNTs materials. As written in the materials section (3.1.1), such as MWCNTs, that the purity of it is 95%, so the 5% contain other aromatic compounds and amorphous carbon. These materials could remain in the solution, and then this part disturbs the PL intensity measurement and gave negative

effect on the adsorption process of SMT on the CNTs. Furthermore, in the sample preparation methods, although centrifugation was used to separate the solution which contain the free SMT in the supernatants from the CNTs, but this method is probably not enough to remove all the CNTs from the solution. Despite our efforts, we did not find the right filter to work around this problem with a filtration step before the measurements. Fortunately, HPLC measurements solved this problem with the separation of the different materials on the column. Accordingly, HPLC was recommended for more precise measurements.

In this work systematic analyses have been done to investigate the effect of the number of layers of walls and the effect of the functionalization of the CNTs. Therefore, five different types of CNTs were used as adsorbent of the SMT molecules to compare their adsorption capacity. To determine which CNTs are the most suitable for effective removal of SMT from aqueous solutions by minimized mass of adsorbent, we applied different CNTs with the same mass and used constant concentration of SMT. Under the same conditions, at 298.2 K and at pH 2, 5 or 7 the SMT adsorption have been monitorized. Figure 21 a), b) and c) shows that increasing the amount of CNTs leads to considerable decrease in the presence of SMT in the solution phase. The SWCNTs can start adsorbing with amount less than 0.01 mg, and reaching the equilibrium by adsorbing the maximum amount of SMT using maximum mass 0.4 mg from SWCNTs. Therefore, SWCNTs were found to be the most appropriate CNTs to adsorb SMT, but it is not surprising because SWCNT has the largest specific surface area. Nevertheless, considering the prices of the CNTs, the possible application of the more cost effective functionalized or nonfunctionalized MWCNTs should not be discarded.

#### **4.3.3.1 Adsorption isotherm of SMT on the CNTs**

To obtain the highest adsorption capacity of the five different CNTs, the Langmuir and Freundlich models were applied to explain the difference between the CNTs and the ionization states of the antibiotic SMT (Figure 21b), d) and f)). The data calculated from the fitted isotherms are summarized in Table 5.

The interaction between SMT and CNTs must take place by various molecular level interactions, namely electrostatic interactions, Lewis acid-base, van der Waals

interactions, hydrophobic interactions, hydrogen bonding, electron donor-acceptor interaction and  $\pi$ - $\pi$  interaction. Yang *et al.* found [105] that the main driving force during the adsorption of SMT onto MWCNTs is electrostatic interaction.

**Table 5** a) Langmuir and b) Freundlich model for adsorption isotherm parameters of (SMT) adsorption by SWCNTs, DWCNTs, MWCNTs, H-MWCNTs and C-MWCNTs.  $Q_0$ ,  $K_L$ ,  $K_F$  and  $n^{-1}$  are  $\pm$  SEM

a

SMT-CNTs	pH	$Q_0$ (mg g <sup>-1</sup> )	$K_L$ (L mg <sup>-1</sup> )	R <sup>2</sup>
SMT-SWCNTs	2	426.3 $\pm$ 80.1	0.1 $\pm$ 0.0	0.985
	5	302.5 $\pm$ 33.8	0.2 $\pm$ 0.1	0.977
	7	285.1 $\pm$ 39.0	0.2 $\pm$ 0.1	0.965
SMT-DWCNTs	2	102.1 $\pm$ 25.5	0.1 $\pm$ 0.0	0.921
	5	82.3 $\pm$ 12.2	0.1 $\pm$ 0.0	0.943
	7	49.7 $\pm$ 6.3	0.6 $\pm$ 0.3	0.759
SMT-MWCNTs	2	85.3 $\pm$ 8.3	0.4 $\pm$ 0.2	0.908
	5	81.5 $\pm$ 3.3	0.6 $\pm$ 0.1	0.947
	7	58.5 $\pm$ 3.5	0.7 $\pm$ 0.1	0.878
SMT-H-MWCNTs	2	45.1 $\pm$ 3.6	0.5 $\pm$ 0.2	0.894
	5	91.8 $\pm$ 9.2	0.2 $\pm$ 0.0	0.965
	7	15.0 $\pm$ 1.3	0.5 $\pm$ 0.2	0.858
SMT-C-MWCNTs	2	105.0 $\pm$ 19.7	0.2 $\pm$ 0.1	0.890
	5	111.6 $\pm$ 7.6	0.1 $\pm$ 0.0	0.986
	7	26.8 $\pm$ 1.0	1.1 $\pm$ 0.2	0.955



b

<b>SMT-CNTs</b>	<b>pH</b>	<b><math>K_F</math> (mg g<sup>-1</sup> (Lmg<sup>-1</sup>)<sup>(1/n)</sup>)</b>	<b><math>n^{-1}</math></b>	<b>R<sup>2</sup></b>
<b>SMT-SWCNTs</b>	2	31.1±2.0	0.7±0.0	0.995
	5	54.5±7.0	0.6±0.1	0.970
	7	49.5±8.5	0.6±0.1	0.945
<b>SMT-DWCNTs</b>	2	10.5±2.6	0.6±0.1	0.938
	5	11.9±2.1	0.5±0.1	0.954
	7	18.3±4.4	0.3±0.1	0.738
<b>SMT-MWCNTs</b>	2	26.3±5.2	0.4±0.1	0.873
	5	36.6±6.6	0.3±0.1	0.771
	7	23.0±4.1	0.3±0.1	0.788
<b>SMT-H-MWCNTs</b>	2	16.8±1.3	0.3±0.0	0.966
	5	13.3±2.6	0.6±0.1	0.954
	7	5.8±1.2	0.3±0.1	0.752
<b>SMT-C-MWCNTs</b>	2	18.3±3.7	0.5±0.1	0.936
	5	17.4±2.4	0.5±0.1	0.970
	7	13.7±1.8	0.2±0.1	0.784

In our present case, the maximum adsorption of SMT on CNTs was 426.3 mg g<sup>-1</sup> at pH 2 using SWCNTs. The reason is attributed to the combination of the large surface area of the SWCNTs and the electrostatic interaction controlled by ionic states of SMT. In good agreement with the adsorption properties of oxytetracycline and ciprofloxacin onto CNTs [96], our results show the adsorption sequence of CNTs in the presence of SMT is as follows SWCNTs > DWCNTs > MWCNTs.

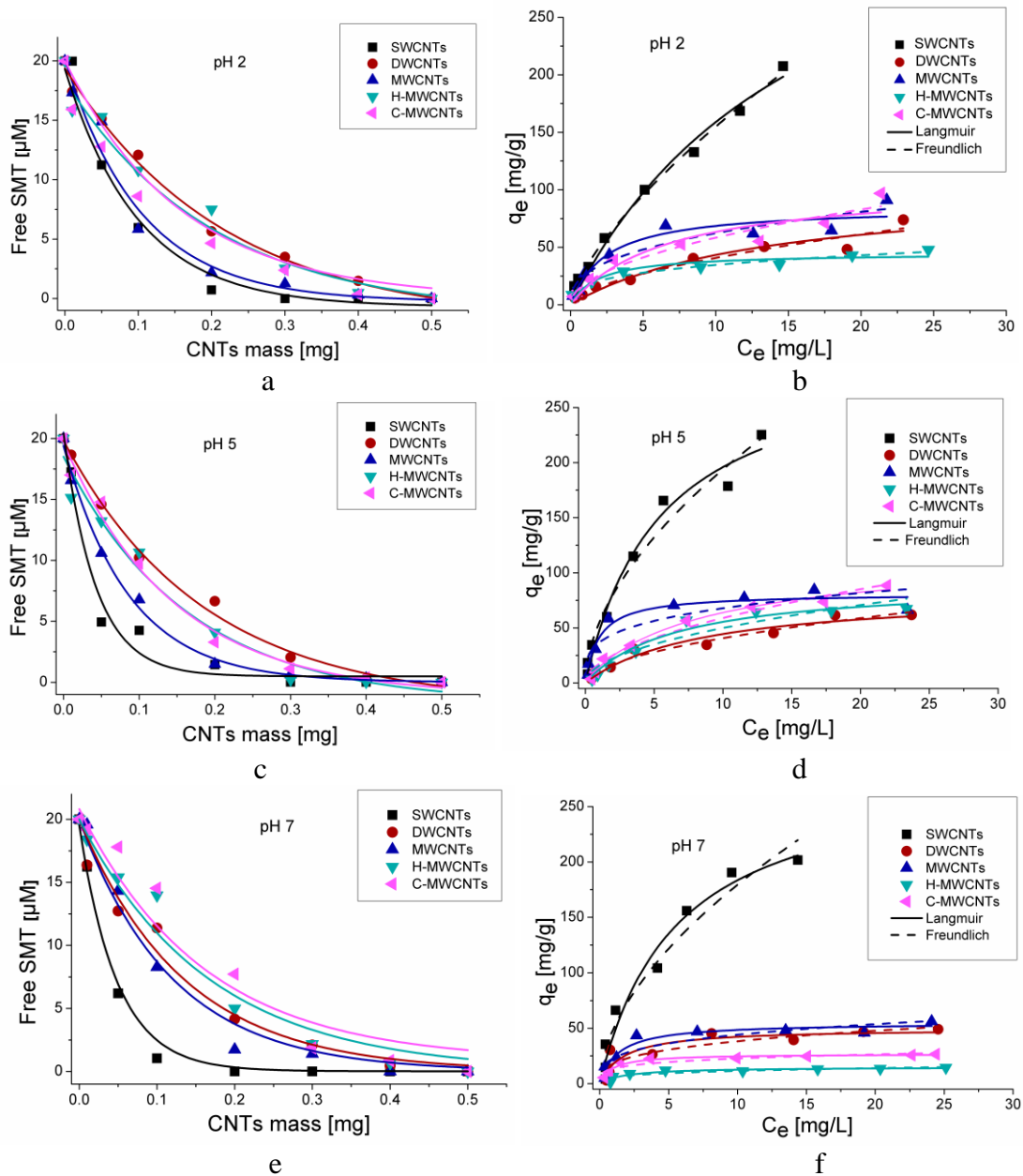


**Figure 21** Extraction of SMT from aqueous solution using SWCNTs, DWCNTs, MWCNTs, H-MWCNTs or C-MWCNTs. Effect of increasing amount of CNTs (0.00, 0.01, 0.05, 0.10, 0.20, 0.30, 0.40 and 0.50 mg/1.5 mL) on the SMT (initial concentration 20  $\mu\text{M}$ ) content of phosphate buffer a) at pH 2 c) pH 5 and e) pH 7. Langmuir and Freundlich isotherms for the SMT adsorption onto CNTs in phosphate buffer b) at pH 2 d) pH 5 and f) pH 7

pH also influences the adsorption properties of SMT onto CNTs. SMT has different protonation form at different pH, while the pH changes play a key role in surface charge characteristics of the adsorbent. According to currently reported data in the

literature, on the nanosurface the SMT is in ionic forms, namely cationic, zwitterionic and anionic controlling by pH [104]. It means, at pH 2, where the cationic and neutral forms are presented in the solution phase, cationic and zwitterionic forms are adsorbed onto the CNTs' surface. Regarding the acidic condition, the electrostatic interaction and hydrogen bonding would be increased due to the increment of the hydrophobicity, solubility and ionization of antibiotics, but SWCNTs are the maximum adsorption capacity due to their large surface area and the highest electrostatic interaction [145]. At pH 5, where the SMT is in the neutral form in the solution phase, the adsorption capacity is lower than at pH 2. At pH 7 the adsorption capacity is the lowest because of the electrostatic repulsion between the negatively charged surface of the adsorbent and the anionic antibiotic presented at a significant amount under these environmental conditions [146]. Furthermore, DWCNTs and MWCNTs play the same role as SWCNTs, which means the best pH for removal SMT in order are  $\text{pH } 2 > \text{pH } 5 > \text{pH } 7$ . These results are in agreement with the earlier reported findings that the increase of the pH decreases the adsorption of SAs [147,98].

The effect of the CNTs' functionalization also has considered and reduced adsorption capacity has been found in the case of H-MWCNTs. Earlier findings [105] showed that the functional -OH groups reduce the hydrophobicity of the CNTs, which is considered as one of the mechanisms controlling the drug adsorption onto the CNTs. Moreover, the phosphate buffer solution includes many ions that can interact with the functional group. When the functional group adsorbs both sodium and potassium ions, they may increase the diffusion resistance and inhibit the drug adsorption onto the CNTs surface [148, 149]. Furthermore, the water solvent molecules surrounding the CNTs' surface may form a solvent shell around the functional group, which also reduces the adsorption capacity of CNTs [150]. Comparing H-MWCNTs and C-MWCNTs the lower adsorption capacity of H-MWCNTs because -OH decrease the hydrophobic interaction with SMT less than -COOH group [151] and -COOH makes C-MWCNTs an electron acceptor, as long as, -OH group makes H-MWCNTs an electron donor resulting an enhanced adsorption capacity of C-MWCNTs [152].

# Chapter 5

---

## 5 Conclusions

Sulfamethazine is a member of sulfonamides antibiotic group containing sulfanilic amide groups, which is used to treat humans and animals to prevent certain infections and improve their antibacterial ability. Unfortunately, this type of drug is poorly soluble in aqueous solution, and the transferring of the sulfonamide in the living body systems by encapsulation with molecules such as BCDs improves the efficacy of the drug. Many efforts have been made but the details about the properties of the drug were missing. To get deeper insight into the encapsulation processes, pH and temperature dependence of the interactions of SMT with the native and randomly methylated BCDs at a wide pH range (2-10) have been investigated using optical spectroscopic methods and molecular modeling calculations. Our major observations and conclusions are the following:

- Sulfamethazine formed weak but stable complexes ( $\log K \sim 3$ ) with native and randomly methylated  $\beta$ -cyclodextrin under different environmental conditions. Although the functionalization of the  $\beta$ -cyclodextrin host molecule by methyl groups does not affect considerably the complex stabilities, the association constants differ significantly only between acidic conditions (pH 2) and at elevated pH (5-10). Based on this finding the relationship between the estimated complex stabilities at room temperature are the following:  $SMT^+ - BCD \sim SMT^+ - RAMEB < SMT^0 - BCD \sim SMT^0 - RAMEB \sim SMT^- - BCD \sim SMT^- - RAMEB$ .
- From the thermodynamic point of view both the spectroscopic measurements and the molecular modeling studies highlight the importance of the reorganization of the solvent molecules. Furthermore, the values of thermodynamic parameters are affected not only by the desolvation of the species interacted but also by the different kinds of noncovalent interactions

(electrostatic interaction, van der Waals interaction, hydrophobic interaction, hydrogen bonding). The presence of competition of the noncovalent interactions and hydration/dehydration processes was confirmed by the analysis of enthalpy – entropy compensation.

- pH-affected structures of the complexes have been found: the sulfamethazine molecule enters into the cyclodextrin cavity with its aromatic amine moiety or with its methyl substituents at low or higher pH, respectively. This result explains the contradictory findings of the complex structures published earlier.
- Molecular modeling calculations indicate the possible tautomerization of sulfamethazine molecule after entering into the randomly methylated  $\beta$ -cyclodextrin cavity. The formation of zwitterionic sulfamethazine in the host cavity has been supported experimentally by FT-IR measurements.

Moreover, SMT considered as one of the environmental pollutants, particularly in the waste water and drink water. SMT extraction from aqueous solution has been tested with the assistance of two different nanomaterials: based on the interaction of SMT with BCD, BBP, an insoluble BCD containing polymer, was tested as the possible SMT binder. Furthermore, CNTs used for the removal of inorganic and organic compounds and SMT adsorption has also been detected by the adsorbent CNTs. Therefore, to investigate the properties of their interaction, systematic analyses of SMT adsorption have been carried out by 5 types of CNTs. The effect of the number of layers of the CNTs' walls and the functionalization of the CNTs have been described. Our major observations and conclusions are the following:

- The insoluble  $\beta$ -cyclodextrin bead polymer is not applicable to remove SMT from aqueous solution effectively. The sulfamethazine-binding ability of this polymer was significantly lower than it was expected on the basis of stability of SMT – BCD complex.
- Carbon nanotubes are capable of effectively decreasing the SMT content of aqueous solution in pH 2, 5, and 7. According to the pH the following order of efficiency for the removal of sulfamethazine from aqueous solution was found: pH 2 > pH 5 > pH 7. The electrostatic interaction between the SMT molecule and carbon nanotube surface is known to be the driving force of the adsorption,

therefore the adsorption of cationic and neutral forms of the drug molecule are higher than the anionic form.

- Both functionalization and the increase of the side wall of the nanotubes decrease their adsorption capacity. Therefore, among the 5 different types of carbon nanotubes investigated, the SWCNT is the most suitable to extract SMT from aqueous media under the range of the environmental conditions investigated.

Based on the findings above my plans for the future works are: to carry out similar investigations for the wide spectra of sulfonamide family. To get a good comparison between the sulfonamide family members, especially sulfonamide derivatives at different pH and temperatures experimentally and theoretically will be studied in addition to their adsorption capacity on the surface of different types of CNTs.

These observations might be relevant for the preparation of orally administered products of sulfonamide-cyclodextrin complexes and they can be useful remove these drugs from contaminated beverages e.g. from drink water.

## 6 References

- 
- [1] Bani-Yaseen. A.D., Mo'ala, A. Spectral, thermal, and molecular modeling studies on the encapsulation of selected sulfonamide drugs in  $\beta$ -cyclodextrin nanocavity, *Spectrochim. Acta A Mol. Biomol. Spectrosc.*, 131 (2014) 424-431
- [2] Li, Y. Thermodynamic studies on a few factors influencing the formations of some representative host-guest complexes, PhD dissertation, University of Pécs, (2014) 88p
- [3] Rajendiran, N., Siva, S., Saravanan, J. Inclusion complexation of sulfapyridine with  $\alpha$ - and  $\beta$ -cyclodextrins: spectral and molecular modeling study, *J. Mol. Struct.*, 1054–1055 (2013) 215-222
- [4] Bhalla, V. Supramolecular chemistry from molecule to molecular machines, *Resonance*, 23(3) (2018) 277-290
- [5] Bani-Yaseen. A. D. Spectrofluorimetric study on the interaction between antimicrobial drug sulfamethazine and bovine serum albumin, *J. Lumin.*, 131 (2011) 1042-1047
- [6] Ma. X., Zhao. Y. Biomedical applications of supramolecular systems based on host-guest interactions, *Chem. Rev.*, 115 (2015) 794-7839
- [7] Wenz. G., Hang. B., Muller. A. Cyclodextrin rotaxanes and polyrotaxanes, *Chem. Rev.*, 106 (2006) 782-817
- [8] Schalley. C. Analytical methods in supramolecular chemistry, *Wiley*, 1 (2012) 844p
- [9] Loftsson, T., Duchêne, D. Cyclodextrins and their pharmaceutical applications, *Int. J. Pharm.*, 329 (2007) 1-11
- [10] Li, S., Purdy, W. C., Cyclodextrins and their applications in analytical chemistry, *Chem. Rev.*, 92 (1992) 1457-1470
- [11] Villalonga, R., Cao, R., Frago, A. Supramolecular chemistry of cyclodextrins in enzyme technology, *Chem. Rev.*, 107 (2007) 3088-3116
- [12] Breslow, R., Dong, S. D. Biomimetic reactions catalyzed by cyclodextrins and their derivatives, *Chem. Rev.*, 98 (1998) 1997-2011

- 
- [13] Davis, M. E., Brewster, M. E. Cyclodextrin-based pharmaceuticals: past, present and future, *Nat. Rev. Drug Discovery*, 3 (2004) 1023-1035
- [14] McCormack, B., Gregoriadis, G. Entrapment of cyclodextrin-drug complexes into liposomes: potential advantages in drug delivery, *J. Drug Targeting*, 2 (1994) 449-454
- [15] Loftsson, T. Effects of cyclodextrins on the chemical stability of drugs in aqueous solutions, *J. Ijpharm.*, 531(2) (2017) (1995) 532-542
- [16] Szente, L., Szejtli, J. Highly soluble cyclodextrin derivatives. Chemistry, properties, and trends in development, *Adv. Drug Deliv.*, 36 (1999) 17-28
- [17] Loftsson, T., Stefánsson, E. Cyclodextrins in eye drop formulations: enhanced topical delivery of corticosteroids to the eye, *Acta. Ophthalmol. Scand.*, 80 (2) (2002) 144-150
- [18] Challa, R., Ahuja, A., Ali, J., and Khar, R. K. Cyclodextrins in drug delivery: an updated review, *AAPS. Pharmsci. Tech.*, 6 (2005) 329-357
- [19] Stella, V. J., He. Q. Cyclodextrins, *Toxicol. Pathol.*, 36 (2008) 30-42
- [20] Loh, X. J. Supramolecular host-guest polymeric materials for biomedical applications, *Mater. Horiz*, 1 (2014) 185-195
- [21] Rekharsky, M. V., Inoue, Y. Complexation thermodynamics of cyclodextrins, *Chem. Rev.*, 98 (1998) 1875-1917
- [22] Rekharsky, M. V.; Inoue, Y. Chiral recognition thermodynamics of  $\beta$ -cyclodextrin: the thermodynamic origin of enantioselectivity and the enthalpy-entropy compensation Effect, *J. Am. Chem. Soc.*, 122 (2000) 4418-4435
- [23] Irie, T., Uekama, K. Cyclodextrins in peptide and protein delivery, *Adv. Drug Delivery Rev.*, 36 (1999) 101-123
- [24] Nepogodiev, S. A. Cyclodextrin-based catenanes and rotaxanes, Stoddart, J. F. *Chem. Rev.*, 98 (1998) 1959-1976
- [25] Liu, L., Guo, Q. X. The driving forces in the inclusion complexation of cyclodextrins, *J. Inclusion Phenom. Macrocyclic Chem.*, 42 (2002) 1-14
- [26] Yasuda, S., Miyake, K., Sumaoka, J., Komiyama, M., Shigekawa, H. Effect of the dipole-dipole interaction on the self-assembly of cyclodextrin inclusion complexes, *Jpn. J. Appl. Phys, Part 1*, 38 (1999) 3888-3891



- 
- [27] Irie, T., Uekama, K. Pharmaceutical applications of cyclodextrins. III. Toxicological issues and safety evaluation, *J. Pharm. Sci.*, 86 (2) (1997) 147-162
- [28] Natesan, S., Enoch, L. V. M. V. Molecular encapsulation of Valganciclovir by  $\beta$ -cyclodextrin influences its binding to bovine serum albumin: a spectroscopic study, *Phys. Chem. Liq.*, 57 (2019) 43-54
- [29] Jansook, P., Ogawa, N., Loftsson, T. Cyclodextrins: structure, physicochemical properties and pharmaceutical applications, *Int. J. Pharm.*, 535 (2018) 272-284
- [30] Jacobsen, A. M., Halling-Sørensen, B., Ingerslev, F., Hansen, S. H. Simultaneous extraction of tetracycline, macrolide and sulfonamide antibiotics from agricultural soils using pressurised liquid extraction, followed by solid-phase extraction and liquid chromatography-tandem mass spectrometry, *J. Chromatogr.*, 1038 (2004) 157-170
- [31] Chen, H., Liu, X., Dou, Y., He, B., Liu, L., Wei, Z., Li, J., Wang, C., Mao, C., Zhang, J., Wang, G. A pH-responsive cyclodextrin-based hybrid nanosystem as a nonviral vector for gene delivery, *Biomaterials*, 34 (2013) 4159-4172
- [32] Zhang, M., Jiang, M., Meng, L., Liu, K., Mao, Y., Yi, T. Fabrication of multiplicate nanostructures via manipulation of the self-assembly between an adamantane based gelator and cyclodextrin, *Soft Matter*, 9 (2013) 9449- 9454
- [33] Tabushi, I. cyclodextrin catalysis as a model for enzyme action, *Acc. Chem. Res.*, 15 (1982) 66-72
- [34] Saenger, W. Angew. Cyclodextrin inclusion compounds in research and industry, *Angew. Chem., Int. Ed. Engl.*, 19 (1980) 344-362
- [35] M. Poór, A. Zand, L. Szente, B. Lemli, S. Kunsági-Máté. Interaction of  $\alpha$ - and  $\beta$ -zearalenols with  $\beta$ -cyclodextrins, *Molecules*, 22 (2017) 1910-1924
- [36] Wenz, G. Cyclodextrins as building blocks for supramolecular structures and functional nits, *Angew. Chem., Int. Ed. Engl.*, 33 (1994) 803-822
- [37] Easton, C. J., Lincoln, S. F. Modified cyclodextrins: scaffolds and templates for supramolecular chemistry; imperial college press: London, 1999
- [38] Rajendiran, N., Mohandoss, T., Venkatesh, G. Investigation of inclusion complexes of sulfamerazine with  $\alpha$ - and  $\beta$ -cyclodextrins: an experimental and

- 
- theoretical study, *Spectrochim. Acta A Mol. Biomol. Spectrosc.*, 124 (2014) 441-450
- [39] Cadars, S., Foray, M. F., Gabelle, A., Gerbaud, G., Bardet, M. High-resolution solid-state  $^{13}\text{C}$  NMR study of per(3,6-anhydro)- cyclodextrin based polymers and of their chromium complexes, *Carbohydr. Polym.*, 61 (2005) 88-94
- [40] Yamasaki. H., Makihata. Y., Fukunaga. K. Preparation of crosslinked  $\beta$ -cyclodextrin polymer beads and their application as a sorbent for removal of phenol from wastewater, *J. Chem. Technol. Biotechnol.*, 83 (2008) 991-997
- [41] Fliszár-Nyúl, E., Lemli, B., Kunsági-Máté, S., Szente, L., Poór, M. Interactions of mycotoxin alternariol with cyclodextrins and its removal from aqueous solution by beta-cyclodextrin bead polymer, *Biomolecules*, 9 (2019) 428-446
- [42] Roston, E. The carbon age. How life's core element has become civilization's greatest threat. New York: Walker & Co., (2009)
- [43] Iijima, S., Helical microtubules of graphitic carbon, *Nature*, 354 (1991) 56-58
- [44] Bagheri, Z. On the utility of C<sub>24</sub> fullerene framework for Li-ion batteries: quantum chemical analysis, *Appl. Surf. Sci.*, 383 (2016) 294-299
- [45] Sun, H., Wang, Q., Guo, Y., Li, B., Li, Y., Yang, Y. Single-handed helical carbonaceous nanotubes prepared using a pair of cationic low molecular weight gelators, *Mater. Res. Bull.*, 80 (2016) 316-320
- [46] In, J. B., Noy, A. Chapter 3. Nanotechnology's wonder material: synthesis of carbon nanotubes, In: Ko SH, Grigoropoulos CP, editors. Hierarchical nanostructures for energy devices, Cambridge: Roy. Soc. Ch., (2014) 26-58
- [47] Bianco, A., Kostarelos, K., Prato, M. Applications of carbon nanotubes in drug delivery, *Curr. Opin. Chem. Biol.*, 9 (2005) 674-679
- [48] Zhang, R., Zhang, Y., Zhang, Q., Xie, H., Qian, W., Wei, F. Growth of half-meterlong carbon nanotubes based on Schulz-Flory distribution, *A. C. S. Nano*, 7 (2013) 6156-6161
- [49] Suzuki, S., Syntheses and applications of carbon nanotubes and their composites, *Intech*, 6 (2013) 118-143

- 
- [50] Zaytseva, O., Neumann, G. Carbon nanomaterials: production, impact on plant development, agricultural and environmental applications, *Chem. Biol. Technol. Agric.*, 3 (2016) 17-43
- [51] Xu, J., Cao, Z., Zhang, Y., Yuan, Z., Lou, Z., Xu, X., Wang, X. A review of functionalized carbon nanotubes and graphene for heavy metal adsorption from water: preparation, application, and mechanism, *Chemosphere*, 195 (2018) 351-364
- [52] Saito, R., Fujita, M., Dresselhaus, G., Dresselhaus, M. S. Electronic structure of chiral graphene tubules, *Appl. Phys. Lett.*, 60 (1992) 2204-2206
- [53] Peles-Lemli, B., Peles-Lemli, J., Kollár, L., Nagy, G., Kunsági-Máté, S. Temperature-independent longitudinal waves obtained on carbon nanotubes with special emphasis on the tubular ion-transport, *Studia Universitatis Babeş-Bolyai. Chemia*, 53 (2) (2008) 37-41
- [54] Yao, Y., Ma, C., Wang, J., Qiao, W., Ling, L., Long, D. Rational design of high surface-area carbon nanotube/microporous carbon core-shell nanocomposites for supercapacitor electrodes, *ACS Appl. Mater. Interfaces*, 7 (2015) 4817-4825
- [55] Jastrzebska, A. M., Karcz, J., Letmanowski, R., Zabost, D., Ciecierska, E., Zdunek, J., Karwowska, E., Siekierski, M., Olszyna, A., Kunicki, A. Synthesis of the RGO/Al<sub>2</sub>O<sub>3</sub> core-shell nanocomposite flakes and characterization of their unique electrostatic properties using zeta potential measurements, *Appl. Surf. Sci.*, 362 (2016) 577-594
- [56] Li, Y., Li, H., Petze, A., Kunsági-Máté, S. Reducing structural defects and improving homogeneity of nitric acid treated multi-walled carbon nanotubes, *Carbon*, 93 (2015) 515-522
- [57] Dresselhaus, M. S., Dresselhaus, G., Charlier, J. C., Hernández, E. Electronic, thermal and mechanical properties of carbon nanotubes, *Phil. Trans. R. Soc. A.*, 362 (2004) 1823-2065
- [58] Popov V., N. Carbon nanotubes: properties and application, *Mat. Sci. Eng. R.*, 43 (3) (2004) 61-102

- 
- [59] Kalra, A., Hummer, G., Garde, S., Methane partitioning and transport in hydrated carbon nanotubes, *J. Phys. Chem. B.*, 108 (2004) 544-549
- [60] Peles-Lemli, B., Matisz, G., Kelterer, A. M., Fabian, W. M. F., Kunsági-Máté, S. Noncovalent interaction between aniline and carbon nanotubes: effect of nanotube diameter and the hydrogen-bonded solvent methanol on the adsorption energy and the photophysics, *J. Phys. Chem., C*, 114 (2010) 5898-5905
- [61] Salipira, K. L., Mamba, B. B., Krause, R. W. Malefetse, T. J., Durbach, S. H. Carbon nanotubes and cyclodextrin polymers for removing organic pollutants from water, *Environ. Chem. Lett.*, 5 (2007) 13-17
- [62] Akhavan, B., Jarvis, K., Majewski, P. Plasma polymer-functionalized silica particles for heavy metals removal, *ACS Appl. Mater. Interfaces*, 7 (2015) 4265-4274
- [63] Lavoie, R. A., Kyser, T. K., Friesen, V. L., Campbell, L. M. Tracking overwintering areas of fish-eating birds to identify mercury exposure, *Environ. Sci. Technol.*, 49 (2015) 863-872
- [64] Ji, L., Chen, W., Zheng, S., Xu, Z., Zhu, D. Adsorption of sulfonamide antibiotics to multiwalled carbon nanotubes, *Langmuir*, 25 (19) (2009) 11608-11613
- [65] Carlson M. S, Fangman T. J. Swine antibiotics and feed additives: food safety considerations, Agricultural Publication G2353, University of Missouri-Columbia: MU. Extension, (2000)
- [66] Jayachandran, S., Lleras-Muney, A., V. Smith, K. Modern medicine and the twentieth century decline in mortality: evidence on the impact of sulfa drugs, *Am. Econ. J-Appl. Econ.*, 2 (2010) 118-146
- [67] Jiménez, V., Adrian, J., Guiteras, J., Marco, M.P., Companyó, R. Validation of an enzyme-linked immunosorbent assay for detecting sulfonamides in feed resources, *J. Agric. Food. Chem.*, 58 (2010) 7526-7531
- [68] Qiang, Z., Adams, C. Potentiometric determination of acid dissociation constants ( $pK_a$ ) for human and veterinary antibiotics, *J. Water Res.*, 38 (2004) 2874-2890

- 
- [69] Cai, Z. X., hang, Y. Z., Pan, H. F., Tie, X. W., Ren, Y. P. Simultaneous determination of 24 sulfonamide residues in meat by ultra-performance liquid chromatography tandem mass spectrometry, *J. Chromatogr.*, 1200 (2008) 144-155
- [70] Koizumi, T., Arita, T., Kakemi, K. Absorption and excretion of drugs. XIX. Some pharmacokinetic aspects of absorption and excretion of sulfonamides. (1). Absorption from rat stomach, *Chemical. Pharm. Bulletin*, 12 (4) (1964) 413–420
- [71] Uekama, K., Hirayama, F., Otagiri, M., Otagiri, Y., Ikeda, K. Inclusion complexation of  $\beta$ -cyclodextrin with some sulfonamides in aqueous solution, *Chemical. Pharm. Bulletin*, 26 (4) (1978) 1162-1167
- [72] Rajendiran, N.; Siva, S. Inclusion complex of sulfadimethoxine with cyclodextrins: preparation and characterization, *Carbohydr. Polym.*, 101 (2014) 828-836
- [73] Semba, T., Funahashi, Y., Ona, N., Yamamoto, Y., Sugi, N. H., Asada, M., Yoshimatsu, K., Wakabayashi, T. An angiogenesis inhibitor E7820 shows broad-spectrum tumor growth inhibition in a xenograft model, *Clin. Cancer Res.*, 10 (2004) 1430-1438
- [74] Slawinski, J., Gdaniec, M. Synthesis, molecular structure, and in vitro antitumor activity of new 4-chloro-2-mercaptobenzenesulfonamide derivatives, *Eur. J. Med. Chem.*, 40 (2005) 377-389
- [75] Chen, Q., Rao, P.N.P., Knaus, E. E. Design, synthesis, and biological evaluation of N-acetyl-2 carboxybenzenesulfonamides: a novel class of cyclooxygenase-2 (COX-2) inhibitors, *Bioorg. Med. Chem.*, 13 (2005) 2459-2468
- [76] Msagati, T. A. M., Nindi, M. M., Multiresidue determination of sulfonamides in a variety of biological matrices by supported liquid membrane with high pressure liquid chromatography-electrospray mass spectrometry detection, *Talanta*, 64 (2004) 87-100
- [77] Chilajwar, S. V., Pednekar, P. P., Jadhav, K. R., Gupta, G. J., Kadam, V. J. Cyclodextrin-based nanosponges: a propitious platform for enhancing drug delivery, *Expert Opin. Drug Del.*, 11 (2014) 111-120

- 
- [78] Zoppi, A., Delviro, A., Aissa, V., Longhi, M. R. Binding of sulfamethazine to  $\beta$ -cyclodextrin and methyl- $\beta$ -cyclodextrin, *AAPS. Pharm. Sci. Tech.*, 14 (2013) 727-735
- [79] Li, B., Meng, Z., Li, Q., Huang, X., Kang, Z., Dong, H., Chen, J., Sun, J., Dong, Y., Li, J., Jia, X., Sessler, J. L., Meng, Q., Li, C. A pH responsive complexation-based drug delivery system for oxaliplatin, *Chem. Sci.*, 8 (2017) 4458- 4464
- [80] Adams, C., Qiang, Z., Barnes, E., Kurwadkar, S., Meyer, M. Occurrence and control of sulfonamides and macrolides antibiotics in full-scale drinking water treatment plants. In: proceedings of the third international conference on pharmaceuticals and endocrine disrupting chemicals in water, Minneapolis, MN, USA, (2003)
- [81] Halling-Sorensen, B., Nors Nielsen, S., Lanzky, PF., Ingerslev, F., Holten Lutzhoft, HC., Jorgensen, SE. Occurrence, fate and effects of pharmaceutical substances in the environment- a review, *Chemosphere*, 36 (1998) 357-393
- [82] Yagub, M.T., Sen, T.K., Afroze, S., Ang, H.M. Dye and its removal from aqueous solution by adsorption: a review, *Adv. Colloid Interface Sci.*, 209 (2014) 172-184
- [83] de Araújo, M. V., Vieira, E. K., Silva Lázaro, G., Conegero, L. S., Almeida, L. E., Barreto, L. S., da Costa, N. B. Jr, Gimenez, I. F. Sulfadiazine/hydroxypropyl- $\beta$ -cyclodextrin host-guest system: characterization, phase-solubility and molecular modeling, *Bioorg. Med. Chem.*, 16 (2008) 5788-5794
- [84] Gladys, G., Claudia, G., Marcela, L., The effect of pH and triethanolamine on sulfisoxazole complexation with hydroxypropyl-beta-cyclodextrin, *Eur. J. Pharm. Sci.*, 20 (3) (2003) 285-293
- [85] Granero, G. E., Maitre, M. M., Garnero, C., Longhi, M. R. Synthesis, characterization and in vitro release studies of a new acetazolamide-HP-beta-CD-TEA inclusion complex, *Eur. J. Med. Chem.*, 43 (3) (2008) 464-470
- [86] Pose-Vilarnovo, B., Perdomo-López, I., Echezarreta-López, M., Schroth-Pardo, P., Estrada, E., Torres-Labandeira, J. J. Improvement of water solubility of

- 
- sulfamethizole through its complexation with beta- and hydroxypropyl-beta-cyclodextrin. Characterization of the interaction in solution and in solid state, *Eur. J. Pharm. Sci.* 13 (3) (2001) 325-331
- [87] Saha, S., Roy, A., Roy, M., N. Mechanistic investigation of inclusion complexes of a sulfa drug with  $\alpha$ - and  $\beta$ -Cyclodextrins, *Ind. Eng. Chem. Res.*, 56 (41) (2017) 11672-11683
- [88] Antony Muthu Prabhu, A., Venkatesh, G., Rajendiran, N. Spectral characteristics of sulfa drugs: effect of solvents, pH and  $\beta$ -cyclodextrin, *J. Solution Chem.*, 39 (2010) 1061-1086
- [89] Poór, M., Matisz, G., Kunsági-Máté, S., Derdák, D., Szente, L., Lemli, B. Fluorescence spectroscopic investigation of the interaction of citrinin with native and chemically modified cyclodextrins, *J. Lumin.*, 172 (2016) 23-28
- [90] Zoppi, A., Quevedo, M.A., Delrivo, A., Longhi, M.R. Complexation of sulfonamides with  $\beta$ -cyclodextrin studied by experimental and theoretical methods, *J. Pharm. Sci.*, 99 (7) (2010) 3166-3176
- [91] Hruska, K., Franek, M. Sulfonamides in the environment: a review and a case report, *Veterinarni. Medicina.*, 57 (1) (2012) 1-35
- [92] Gao, Q., Deng, W., Gao, Z., Li, M., Liu, W., Wang, X., Zhu, F. Effect of sulfonamide pollution on the growth of manure management candidate *Hermetia illucens*. *PLOS ONE*, 14 (5) (2019) e0216086
- [93] Han, Y., Yanga, L., Chen, X., Cai, Y., Zhang, X., Qian, M., Chen, X., Zhao, H., Sheng, M., Cao, G., Shen, G. Removal of veterinary antibiotics from swine wastewater using anaerobic and aerobic biodegradation, *Sci. Total Environ.*, 709 (2020) 136094
- [94] Habibizadeh, M., Rostamizadeh, K., Dalali, N., Ramazani, A. Preparation and characterization of PEGylated multiwall carbon nanotubes as covalently conjugated and non-covalent drug carrier: a comparative study, *Mater. Sci. Eng., C*, 74 (2017) 1-9
- [95] Skwarecki, A. S., Milewski, S., Schielmann, M., Milewska, M. J. Antimicrobial molecular nanocarrier-drug conjugates, *Nanomed. Nanotechnol. Biol. Med.*, 12 (6) (2016) 2215- 2240

- 
- [96] Ncibi, M. C., Sillanpää, M. Optimized removal of antibiotic drugs from aqueous solutions using single, double and multi-walled carbon nanotubes, *J. Hazard Mater.*, 298 (2015) 102-110.
- [97] Niu, H., Cai, Y., Shi, Y., Wei, F., Liu, J., Mou, S., Jiang, G. Evaluation of carbon nanotubes as a solid-phase extraction adsorbent for the extraction of cephalosporins antibiotics, sulfonamides and phenolic compounds from aqueous solution, *Anal. Chim. Acta*, 594 (1) (2007) 81-92
- [98] Tian, Y., Gao, B., Chen, H., Wang, Y., Li, H. Interactions between carbon nanotubes and sulfonamide antibiotics in aqueous solutions under various physicochemical conditions, *J. Environ. Sci. Heal. A*, 48 (2013) 1136-1144
- [99] Pan, B., Zhang, D., Li, H., Wu, M., Wang, Z., Xing, B. Increased adsorption of sulfamethoxazole on suspended carbon nanotubes by dissolved humic acid, *Environ. Sci. Technol.*, 47 (14) (2013) 7722-7728
- [100] Wang, F., Ma, S., Si, Y., Dong, L., Wang, X., Yao, J., Chen, H., Yi, Z., Yao, W., Xing, B. Interaction mechanisms of antibiotic sulfamethoxazole with various graphene- based materials and multiwall carbon nanotubes and the effect of humic acid in water, *Carbon*, 114 (2017b) 671-678
- [101] Gutiérrez, M. C., Ferrer, M. L., Mateo, R., del Monte, M. Freeze-drying of aqueous solutions of deep eutectic solvents: a suitable approach to deep eutectic suspensions of self-assembled structures, *Langmuir*, 25 (10) (2009) 5509-5515
- [102] Zhang, D., Pan, B., Zhang, H., Ning, P., Xing, B., Contribution of different sulfamethoxazole species to their overall adsorption on functionalized carbon nanotubes, *Environ. Sci. Technol.*, 44 (10) (2010) 3806-3811
- [103] Lan, Y. K. , Chen, T. C., Tsai, H. J., Wu, H. C., Lin, J. H., Lin, I. K., Lee, J. F., Chen, C.S. Adsorption behavior and mechanism of antibiotic sulfamethoxazole on carboxylic-functionalized carbon nanofibers-encapsulated Ni magnetic nanoparticles, *Langmuir*, 32 (2016) 9530-9539
- [104] Teixidó, M., Pignatello, J. G., Beltran, J. L., Granados, M., Peccia, J. Speciation of the ionizable antibiotic sulfamethazine on black carbon (Biochar), *Environ. Sci. Technol.*, 45 (2011) 10020-10027



- 
- [105] Yang, Q., Chen, G., Zhanga, J., Lic, H. Adsorption of sulfamethazine by multi-walled carbon nanotubes: effects of aqueous solution chemistry, *RSC Adv.*, 5 (2015) 25541-25549
- [106] Kunsági-Máte, S., Csok, Z., Iwata, Z., Szász, E., Kollár, L. Role of the conformational freedom of the skeleton in the complex formation ability of resorcinarene derivatives toward a neutral phenol guest, *J. Phys. Chem. B.*, 115 (13) (2011) 3339-3343
- [107] Kunsági-Máte, S., Kumar, A., Sharma, P., Kollár, L., Nikfardjam, M. P. Effect of molecular environment on the formation kinetics of complexes of malvidin-3-o-glucoside with caffeic acid and catechin, *J. Phys. Chem. B.*, 113 (21) (2009) 7468- 7473
- [108] Poór, M., Kunsági-Máté, S., Sali, N., Kőszegi, T., Szente, L., Lemli, B. Interactions of zearalenone with native and chemically modified cyclodextrins and their potential utilization, *J. Photochem. Photobiol.*, 151 (2015) 63-68
- [109] Benet, L. Z, Goyan, J. E. Potentiometric determination of dissociation constants, *J. Pharm. Sci.*, 56 (1967) 665-680
- [110] Okamoto, J.; Matsubara, T., Kitagawa, T., Umeda, T. Determination of a sulfur-containing drug in human plasma by an improved method for sulfur chemiluminescence detection in combination with capillary gas chromatography, *Anal. Chem.*, 72 (2000) 634-638
- [111] Carignan, G.; Carrier, K. Quantitation and confirmation of sulfamethazine residues in swine muscle and liver by LC and GC/MS, *J. Assoc. Off. Anal. Chem.*, 74 (1991) 479-482
- [112] Lin, C. E., Lin, W. C; Chiou, W. C. Migration behavior and separation of sulfonamides in capillary zone electrophoresis. I. Influence of buffer pH and electrolyte modifier, *J. Chromatogr. A.*, 755 (1996) 261-269
- [113] Bartolucci, G., Pieraccini, G., Villanelli, F., Moneti, G., Triolo, A. Liquid chromatography tandem mass spectrometric quantitation of sulfamethazine and its metabolites: direct analysis of swine urine by triple quadrupole and by ion trap mass spectrometry, *Rapid Commun. Mass spectrom.*, 14 (2000) 967-973

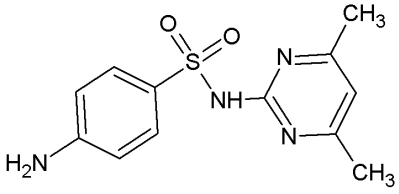
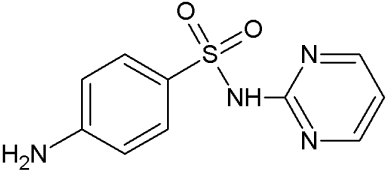
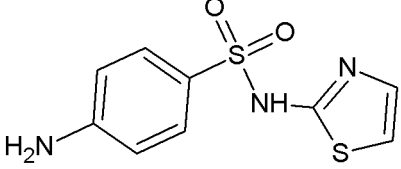
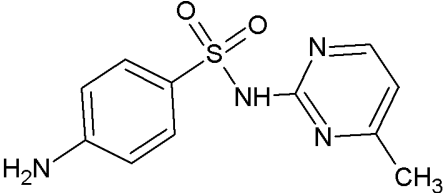
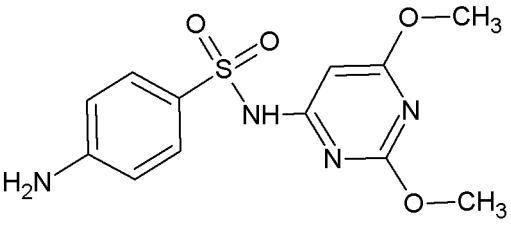
- 
- [114] Leveque, D., Gallion-Renault, C., Monteil, H., Jehl, F. Analysis of recent antimicrobial agents in human biological fluids by high-performance liquid chromatography, *J. Chromatogr. A*, 815 (1998) 163-172
- [115] Maudens, K. E., Zhang, G. F., Lambert, W. E. Lambert, Quantitative analysis of twelve sulfonamides in honey after acidic hydrolysis by high-performance liquid chromatography with post-column derivatization and fluorescence detection, *J. Chromatogr. A*, 1047 (2004) 85-92
- [116] Kishida, K., Furusawa, N. Matrix solid-phase dispersion extraction and high-performance liquid chromatographic determination of residual sulfonamides in chicken, *J. Chromatogr. A*, 937 (1–2, 7) (2001) 49-55
- [117] Muddana, H. S., Gilson, M. K. Calculation of host–guest binding affinities using a quantum-mechanical energy model, *J. Chem. Theory. Comput.*, 8 (2012) 2023-2033
- [118] Fifere, A., Marangoci, N., Maier, S., Coroaba, A., Maftai, D., Pinteala, M. Theoretical study on  $\beta$ -cyclodextrin inclusion complexes with propiconazole and protonated propiconazole, *Beilstein J. Org. Chem.*, 8 (2012) 2191-2201
- [119] Rabello, M. M., Rolim, L. A., Rolim Neto, P., J., Hernandez, M., Z. CycloMolder software: building theoretical cyclodextrin derivatives models and evaluating their host:guest interactions, *J. Incl. Phenom. Macro.*, 93 (2019) 301-308
- [120] Faisal, Z., Kunsági-Máté, S., Lemli, B., Szente, L., Bergmann, D., Humpf, H-U., Poór, M. Interaction of dihydrocitrinone with native and chemically modified cyclodextrins, *J. Molecules*, 24 (2019) 1328-1335
- [121] HyperChem, Hypercube Inc., (2007)
- [122] Papastephanou, C., Frantz, M. Sulfamethazine, *Anal. Profiles. Drug Subst.*, 7 (1978) 401-22
- [123] Lin C. E, Lin W. C, Chen Y. C, Wang S. W. Migration behavior and selectivity of sulfonamides in capillary electrophoresis, *J. Chromatogr. A*, 792 (1997) 37-47
- [124] Alderighi, L., Gans, P., Ienco, A., Peters, D., Sabatini, A., Vacca, A. Hyperquad simulation and speciation (HySS): a utility program for the

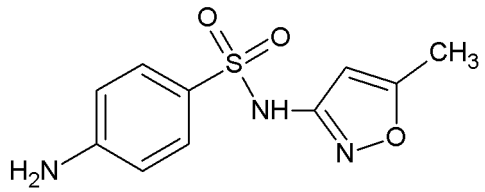
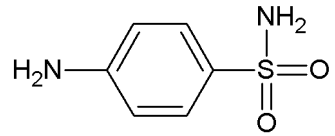
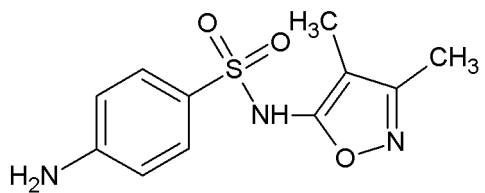
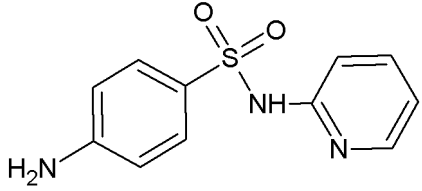
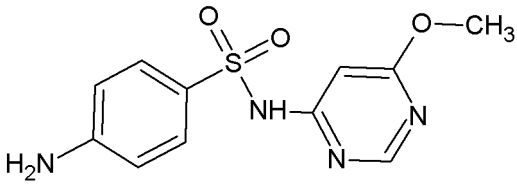
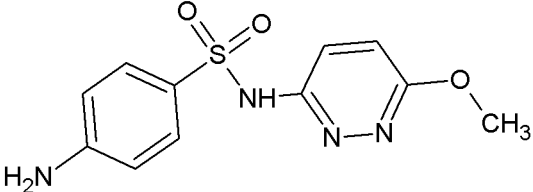
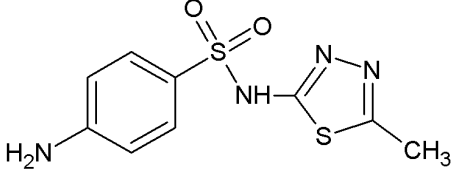
- 
- investigation of equilibria involving soluble and partially soluble species, *J. Coordin. Chem. Rev.*, 184 (1999) 311-318
- [125] Lazar, P., Lee, Y., Kim, S., Chandrasekaran, M., Lee, K. W. Molecular dynamics simulation study for ionic strength dependence of RNA-host factor interaction in staphylococcus aureus Hfq, *Bull. Korean. Chem. Soc.*, 31 (6) (2010) 1519-1526
- [126] Sakurai, H., Ishimitsu, T. Microionization constants of sulphonamides, *Talanta*, 27 (3) (1980) 293-298
- [127] Poór, M., Bálint, M., Hetényi, Cs., Góder, B., Kunsági-Máté, S., Kőszegi, T., Lemli, B. Investigation of non-covalent interactions of aflatoxins (B1, B2, G1, G2 and M1) with serum albumin, *J. Toxins*, 9 (2017) 339-351
- [128] Poór, M., Boda, G., Kunsági-Máté, S., Needs, P. W., Kroon, P. A., Lemli, B. Fluorescence spectroscopic evaluation of the interactions of quercetin, isorhamnetin, and quercetin-3'-sulfate with different albumins, *J. Lumin.*, 194 (2018) 156-163
- [129] Gans, P., Sabatini, A., Vacca, A. Investigation of equilibria in solution. Determination of equilibrium constants with the HYPERQUAD suite of programs, *J. Talanta*, 43 (1996) 1739-1753
- [130] Liu, M., Guo, Q., Shi, Y., Cai, C., Pei, W., Yan, H., Jia, H., Han, J. Studies on pH and temperature dependence of inclusion complexes of bisdemethoxycurcumin with  $\beta$ -cyclodextrin derivatives, *J. Mol. Struct.*, 1179 (2019) 336-346
- [131] Terekhova, I. V., Chislov, M. V., Brusnikina, M. A., Chibunova, E. S., Volkova, T. V., Zvereva, I. A., Proshin, A. N. Thermodynamics and binding mode of novel structurally related 1,2,4-thiadiazole derivatives with native and modified cyclodextrins, *Chem. Phys. Lett.*, 671 (2017) 28-36
- [132] Dragan, A. I., Read, C. M., Crane-Robinson, C. Enthalpy-entropy compensation: the role of solvation, *Eur. Biophys. J.*, 46 (2017) 301-308
- [133] Pan, A., Kar, T., Rakshit, A. K., Moulik, S. P. Enthalpy-entropy compensation (EEC) effect: decisive role of free energy, *J. Phys. Chem. B*, 120 (2016) 10531-10539

- 
- [134] Pan, A., Biswas, T., Rakshit, A. K., Moulik, S. P. Enthalpy-entropy compensation (EEC) effect: a revisit, *J. Phys. Chem. B*, 119 (2015) 15876-15884
- [135] Kunsági-Máté, S.; Iwata, K. Effect of cluster formation of solvent molecules on the preferential solvation of anthracene in binary alcoholic solutions, *Chem. P. L.*, 473 (2009) 284-287
- [136] Kunsági-Máté, S., Iwata, K. Electron density dependent composition of the solvation shell of phenol derivatives in binary solutions of water and ethanol, *J. Solution Chem.*, 42 (2013) 165-171
- [137] Andersson, K. I., Eriksson, M., Norgren, M. Removal of lignin from wastewater generated by mechanical pulping using activated charcoal and fly ash: adsorption isotherms and thermodynamics, *Ind. Eng. Chem. Res.*, 50 (2011) 7722-7732
- [138] Xu, J., Lv, X., Li, J., Li, Y., Shen, L., Zhou, H., Xu, X. Simultaneous adsorption and dechlorination of 2,4-dichlorophenol by Pd/Fe nanoparticles with multiwalled carbon nanotube support, *J. Hazard. Mater.*, (225-226) (2012b) 36-45
- [139] Zhao, H., Liu, X., Cao, Z., Zhan, Y., Shi, X., Yang, Y., Zhou, J., Xu, J. Adsorption behavior and mechanism of chloramphenicols, sulfonamides, and nonantibiotic pharmaceuticals on multi-walled carbon nanotubes, *J. Hazard. Mater.*, 310 (2016) 235-245
- [140] Lee, D., Yang, H., Yan, R., & Liang, D. T. Prediction of gaseous products from biomass pyrolysis through combined kinetic and thermodynamic simulations, *Fuel*, 86 (2007) 410-417
- [141] Mishra, A. K., Ramaprabhu, S. Magnetite decorated multiwalled carbon nanotube based supercapacitor for arsenic removal and desalination of seawater, *J. Phys. Chem. C*, 114 (2010) 2583-2590
- [142] Wan, S., He, F., Wu, J., Wan, W., Gu, Y., Gao, B. Rapid and highly selective removal of lead from water using graphene oxide-hydrated manganese oxide nanocomposites, *J. Hazard. Mater.*, 314 (2016) 32-40

- 
- [143] Myers, A. L. Thermodynamics of adsorption. In chemical thermodynamics for industry; Letcher, T., Ed. R. S. C., London, (2004) 243-253
- [144] Xu, J., Liu, X., Lowry, G.V., Cao, Z., Zhao, H., Zhou, J. L., Xu, X. Dechlorination mechanism of 2,4-dichlorophenol by magnetic MWCNTs supported Pd/Fe nanohybrids: rapid adsorption, gradual dechlorination, and desorption of phenol, ACS Appl. Mater. Interfaces, 8 (2016b) 7333-7342
- [145] Kurwadkar, S. T., Adams, C. D., Meyer, M. T., Kolpin, D. W. Effects of sorbate speciation on sorption of selected sulfonamides in three loamy soils, J. Agric. Food Chem., 55 (2007) 1370-1376
- [146] Lertpaitoonpan, W., Ong, S. K., Moorman, T. B. Effect of organic carbon and pH on soil sorption of sulfamethazine, Chemosphere, 76 (2009) 558-564
- [147] Ahmed, M. B., Zhou, J. L., Ngo, H. H., Guo, W., Mah, J., Belhaj, D. Competitive sorption affinity of sulfonamides and chloramphenicol antibiotics toward functionalized biochar for water and wastewater treatment, Bioresour. Technol., 238 (2017b) 306–312
- [148] Wang, T., Liu, W., Xiong, L., Xu N., Ni, J., Influence of pH, ionic strength and humic acid on competitive adsorption of Pb(II), Cd(II) and Cr(III) onto titanate nanotubes, Chem. Eng. J., (215–216) (2013) 366-374
- [149] Wang, X., Liu, Y., Tao, S., Xing, B. Relative importance of multiple mechanisms in sorption of organic compounds by multiwalled carbon nanotubes, Carbon, 48 (2010) 3721-2728
- [150] Yang, K., Xing, B. Adsorption of organic compounds by carbon nanomaterials in aqueous phase: polanyi theory and its application, Chem. Rev., 110 (2010) 5989-6008
- [151] Ma, X., Uddin, S. Desorption of 1,3,5-trichlorobenzene from multi-walled carbon nanotubes: impact of solution chemistry and surface chemistry, Nanomaterials, 3 (2) (2013) 289-302
- [152] Keiluweit, M., Kleber, M. Molecular-level interactions in soils and sediments: the role of aromatic  $\pi$ -systems, Environ.Sci. Technol., 43 (2009) 3421-3429

## Appendix

<p><b>Sulfonamides</b></p> <p><b>Abbreviations</b></p> <p><b>Structure formulas</b></p> <p><b>pK values</b></p>	<p><b>Structures</b></p>
<p>Sulfamethazine</p> <p><math>C_{12}H_{14}N_4O_2S</math></p> <p><math>pK_{a1}=2.36, pK_{a2}=7.38</math> [70]</p>	
<p>Sulfadiazine</p> <p><math>C_{10}H_{10}N_4O_2S</math></p> <p><math>PK_{a1}=2.0, pK_{a2}=6.37</math> [70]</p>	
<p>Sulfathiazole</p> <p><math>C_9H_9N_3O_2S_2</math></p> <p><math>pK_{a1}=2.01, pK_{a2}=7.11</math> [68]</p>	
<p>Sulfamerazine</p> <p><math>C_{11}H_{11}N_4O_2SNa</math></p> <p><math>pK_{a1}=2.26, pK_{a2}=7.06</math> [70]</p>	
<p>Sulfadimethoxine</p> <p><math>C_{12}H_{14}N_4O_4S</math></p> <p><math>pK_{a1}=2.13, pK_{a2}=6.08</math> [68]</p>	

<p>Sulfamethoxazole</p> <p><math>C_{10}H_{11}N_3O_3S</math></p> <p><math>pK_{a1}=1.85, pK_{a2}=5.6</math> [68]</p>	
<p>Sulfanilamide</p> <p><math>C_6H_8N_2O_2S</math></p> <p><math>pK_{a1}=2.36, pK_{a2}=10.43</math> [70]</p>	
<p>Sulfisoxazole</p> <p><math>C_{11}H_{13}N_3O_3S</math></p> <p><math>pK_{a1}=1.55, pK_{a2}=5.1</math> [70]</p>	
<p>Sulfapyridine</p> <p><math>C_{11}H_{11}N_3O_2S</math></p> <p><math>pK_{a1}=2.58, pK_{a2}=8.43</math> [70]</p>	
<p>Sulfamonomethoxine</p> <p><math>C_{11}H_{12}N_4NaO_3S</math></p> <p><math>pK_{a1}=2.0, pK_{a2}=5.9</math> [70]</p>	
<p>Sulfamethoxypyridazine</p> <p><math>C_{11}H_{12}N_4O_3S</math></p> <p><math>pK_{a1}=2.06, pK_{a2}=6.09</math> [70]</p>	
<p>Sulfamethizole</p> <p><math>C_9H_{10}N_4O_2S_2</math></p> <p><math>pK_{a1}=2.00, pK_{a2}=5.45</math> [70]</p>	

**Table 6** a) The Langmuir and b) Freundlich model fitting adsorption isotherm parameters for adsorption of SMT, sulfapyridine (SPY) and sulfamethoxazole (SMX) by MWCNTs, H-MWCNTs, C-MWCNTs and pristine-MWCNTs (P-MWCNTs).

$Q_0$ ,  $K_L$ ,  $K_F$  and  $n^{-1}$  are  $\pm$  SEM of the ref.

a

SMT-CNTs	pH	$Q_0$ (mg g <sup>-1</sup> )	$K_L$ (L mg <sup>-1</sup> )	R <sup>2</sup>	Ref.
SMT- P-MWCNT	5.0±0.1	38.1±0.6	0.07±0.00	0.995	[105]
SMT- H-MWCNT	5.0±0.1	27.3±0.4	0.04±0.00	0.998	
SMX-*MWCNT	3	98.0	0.2	0.995	[98]
SMX-*MWCNT	5.6	82.2	0.3	0.989	
SMX-*MWCNT	7	48.8	0.2	0.992	
SMX-*MWCNT	9	18.6	0.0	0.987	
Spy-*MWCNT	3	108.6	0.2	0.961	
Spy-*MWCNT	5.6	102.1	0.2	0.974	
Spy-*MWCNT	7	94.5	0.13	0.968	
Spy-*MWCNT	9	83.2	0.2	0.971	

\*functional groups (e.g., carboxyl and hydroxyl groups)



---

b

SMT-CNTs	pH	$K_F$ (mg g <sup>-1</sup> (Lmg <sup>-1</sup> ) <sup>(1/n)</sup> )	$n^{-1}$	R <sup>2</sup>	Ref.
SMT- P-MWCNT	5.0±0.1	6.73±0.8	0.4±0.0	0.947	[105]
SMT- H-MWCNT	5.0±0.1	3.0±0.4	0.5±0.03	0.963	
SMX- H-MWCNT	1	6.0±0.3	1.7±0.02	0.982	[102]
SMX- H-MWCNT	3.7	12.2±0.5	1.9±0.02	0.978	
SMX- H-MWCNT	7.5	0.7±0.03	1.1±0.02	0.980	
SMX- C-MWCNT	1	4.3±0.2	1.7±0.02	0.979	
SMX- C-MWCNT	3.7	6.4±0.4	1.8±0.02	0.963	
SMX- C-MWCNT	7.5	0.4±0.02	0.9±0.02	0.984	

---

## Publication List

### a. Publications in refereed journals related to this thesis

1. Mohamed Ameen, H., Kunsági-Máté, S., Szente, L., Lemli, B. Encapsulation of sulfamethazine by native and randomly methylated  $\beta$ -cyclodextrins: The role of the dipole properties of guests, *Spectrochim. Acta A Mol. Biomol. Spectrosc.*, 225 (2020) 117475
2. Mohamed Ameen, H., Kunsági-Máté, S., Szente, L., Bognár, B., Lemli, B. Thermodynamic characterization of the interaction between an antimicrobial drug sulfamethazine and two selected cyclodextrins, *Molecules*, 24 (2019) 4565
3. Mohamed Ameen, H., Kunsági-Máté, S., Noveczky, P., Szente, L., Lemli, B. Adsorption of sulfamethazine drug onto the modified derivatives of carbon nanotubes at different pH (under review)

### b. Publications in refereed journals not related to this thesis

1. E.AL-Mukhtar, S., F.AL-Katib, H., A.AL-Nuamimy, L. Preparation and characterization of some transition metal complexes with crotyl xanthate ligand and their adducts with nitrogen bases, *J.AL-Rafidane* , 26(1) (2017) 49-55
2. F.AL-Katib, H. A series of M-M heterometallic coordination polymers: syntheses structures properties. *KUJSS*, 1992 (2016) 0849
3. Kiss, L., Mohamed Ameen, H., Lemli, B., Kunsági-Máté, S. Determination of solubility of 4-(2-hydroxyethyl)-1-piperazineethanesulfonic acid and its sodium salt in acetonitrile and voltammetric investigation of sulphonamide drugs in different solvents in their absence and presence (under review)

---

### **c. Posters and presentations related to the thesis**

1. Mohamed Ameen, H., Kunsági-Máté, S., Lemli, B. The effect of pH on the interaction between sulfamethazine and b-cyclodextrin, 3rd Symposium on Weak Molecular Interactions, Poland, Opole, (2017) p11
2. Mohamed Ameen, H., Lemli, B. pH dependent encapsulation of sulfamethazine antibiotic by cyclodextrin derivatives, Med Pecs conference, Hungary, Pecs, (2018) p 41
3. Mohamed Ameen, H., Kunsági-Máté, S., Lemli, B. Encapsulation of selected sulfamethazine by beta cyclodextrin and random methylated beta-cyclodextrin, 3rd International Symposium on Scientific and Regulatory Advances in Biological and Non-Biological Complex Drugs: A to Z in Bioequivalence conference, Hungary, Budapest, (2018) p 13

---

## Acknowledgements

I would like to acknowledge my indebtedness and render my warmest thanks to Dr. Beáta Lemli, my supervisor, , who made this work possible by offering the opportunity to work on such an interesting scientific topic. Her friendly guidance and expert advice have been invaluable throughout all stages of the work.

I would also wish to express my gratitude to Dr. Sándor Kunsági-Máté for the extended discussions and valuable suggestions which have contributed greatly to the improvement of the thesis.

Special thanks are due to my husband, Dr. Maan Al-Fathi, for his continuous support, encouraging and understanding. He helped me with creating the figures and editing the dissertation. My thanks are extended to my brothers and my sister for their constant encouragement.

I would like to thank Dr. Zsolt Preisz for helping me to correct English language in this work.

Thanks are given to Erzsébet Szász, Dr. László Kiss, Dr. Miklós Poór, Diána Derdák, Ferenc Kovács and Kristóf Kecskés for their kind assistance during my experiments.